BRIGHAM YOUNG UNIVERSITY

# GEOLOGY STUDIES

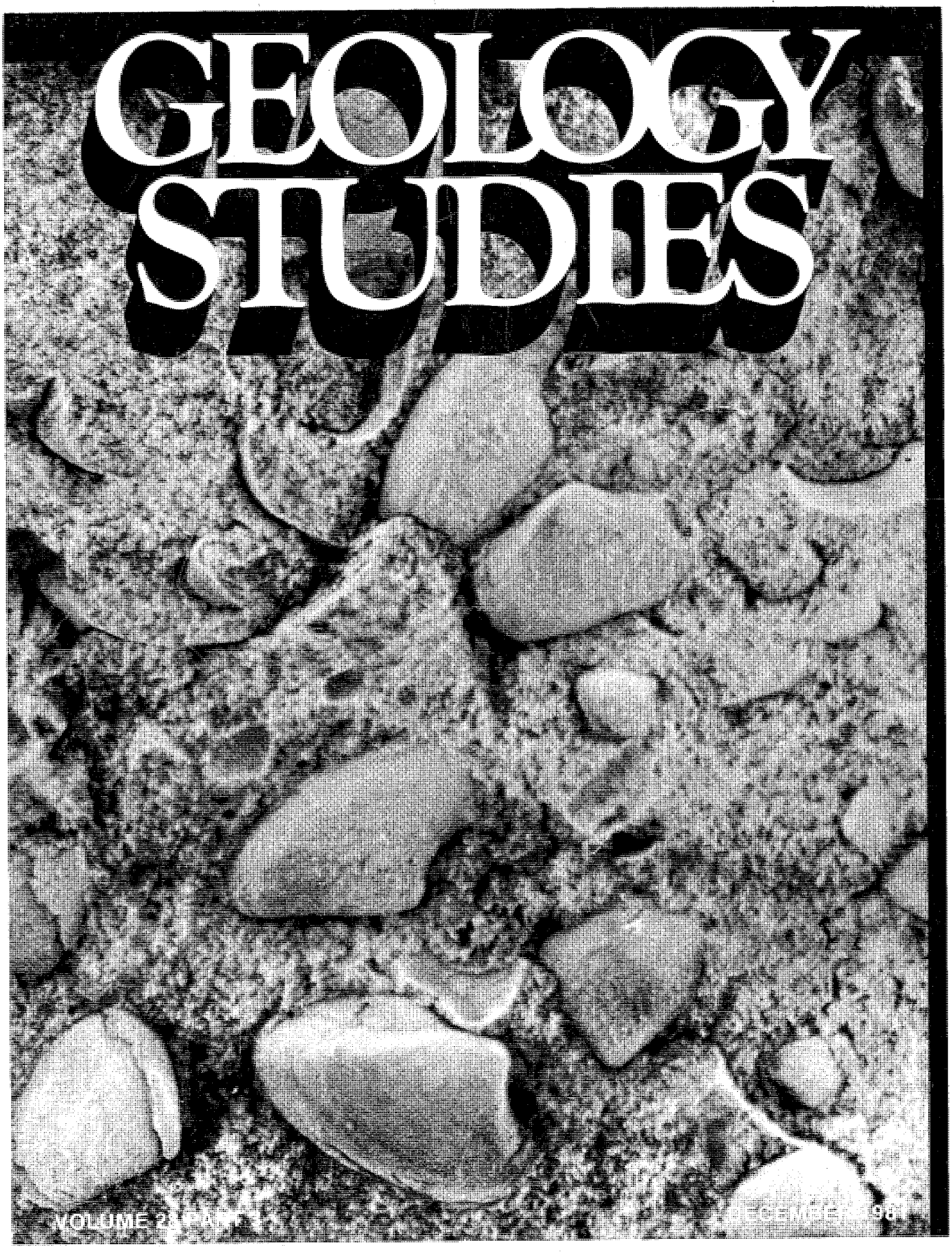

VOLUME 2[illegible] DECEMBER 19[illegible]

# Brigham Young University Geology Studies

## Volume 28, Part 3

## CONTENTS




*Cover: Slab of bivalves showing* Myalina-Pleuroma *suite, from Torrey section, Sinbad Limestone Member, Moenkopi Formation in the Teasdale Dome Area, Wayne County, Utah. Photo courtesy James Scott Dean.*

A publication of the
Department of Geology
Brigham Young University
Provo, Utah 84602

Editors

W. Kenneth Hamblin
Cynthia M. Gardner

*Brigham Young University Geology Studies* is published by the Department of Geology. This publication consists of graduate student and faculty research within the department as well as papers submitted by outside contributors. Each article submitted by BYU faculty and outside contributors is externally reviewed by at least two qualified persons.

ISSN 0068-1016

Distributed December 1981

12-81 600 52593

CONTENTS

# Carbonate Petrology and Depositional Environments of the Limestone Member of the Carmel Formation, near Carmel Junction, Kane County, Utah*

DOUGLAS W. TAYLOR
*Union Oil Company*
*P.O. Box 2620*
*Casper, Wyoming 82602*

ABSTRACT.–The limestone member of the Carmel Formation in the Carmel Junction area represents the transgression of a shallow epeiric sea into southern Utah during Middle Jurassic (Bajocian) time. Three depositional phases are recognized in the nine measured sections.

Early transgression during the first phase is characterized by deposition of subaerial sandstones and shales. Thinly laminated, massive, and cryptalgal dolomicrite, as well as stromatolitic boundstone and nodular anhydrite, represent supratidal deposition. Cross-bedded oolitic-skeletal packstones and grainstones suggest intertidal to subtidal deposition on shoals. Burrowed bivalve wackestones indicate subtidal deposition. Pervasive syngenetic dolomitization and a near total lack of fossils document shallow-water hypersaline conditions in supratidal deposits. Abundant oolites, and bivalve, bryozoan, and echinoderm fragments indicate normal marine subtidal limestone deposition.

Deposition during the second phase occurred as the Carmel Sea retreated abruptly. Shale and argillaceous limestone were deposited in shallow lagoonal waters protected by shoals. Absence of fossils suggests inhospitable conditions for marine organisms.

Well-sorted peloidal grainstones of the final phase document a minor reinvasion of the Carmel Sea into the area. Current-laminated grainstones, bivalve coquinas, and isolated gastropods suggest normal marine deposition on shoals of nearly moderate energy prior to deposition of redbeds of the overlying banded member of the Carmel Formation.

## INTRODUCTION AND GEOLOGIC SETTING

The type section area of the Carmel Formation (Bajocian-Callovian) in southwestern Utah provides an excellent opportunity to study the carbonate petrology and depositional environments of the lower limestone member. Exceptional exposures of this Middle Jurassic calcareous sequence crop out on hillsides and in roadcuts near Carmel Junction, as well as to the south and southwest in Parunuweap Canyon along the Virgin River and its tributaries (fig. 1). Completely exposed carbonate units of dolomite and limestone as well as clastic units of shale, siltstone and sandstone document rapid facies changes near the southern end of a shallow epeiric sea (fig. 2). The famed *Pentacrinus* beds of the Carmel limestone member are found within the study area and are associated with a restricted mollusk and bryozoan fauna. The study area lies near the southern edge of the High Plateaus of the Colorado Plateau. The studied sections are on the downthrown side and immediately west of the Sevier Fault. Rocks in the area dip gently to the northeast. Figure 3 shows a typical exposure of the limestone member of the Carmel Formation in the area.

The purpose of this study is to describe the lithology and paleontology of the limestone member and to interpret the carbonate and clastic sedimentary environments represented there. These data will be used to construct a three-dimensional sedimentary model. With the increasing oil and gas exploration along the Utah hingeline, the limestone member of the Carmel Formation is of prime importance as a possible petroleum source, as well as a potential reservoir.

The Carmel Formation is an eastward-thinning limestone, gypsum, and redbed sequence which rests disconformably on the Temple Cap and Navajo Sandstones throughout southern Utah (Peterson and Pipiringos 1979, p. 10). Although nomenclature varies in southern and eastern Utah, the Carmel Formation as a whole consists of four members and is more than 200 m thick in the Carmel Junction area. They are (from oldest to youngest) the limestone member, the banded member, the gypsiferous member, and the Winsor Member.

The limestone member, discussed in detail in this report, consists of dolomitic mudstones; oolitic, argillaceous, and peloidal limestones; and minor clastic units of sandstone, siltstone, and shale. The limestone member averages 70 m thick and forms mostly ledges and cliffs in the area.

The banded member, named for the interbedded light red to light gray fine-grained sandstones, is a slope-forming unit above the limestone member and is approximately 60 m thick.

The gypsiferous member consists of white to light gray thinly bedded gypsum in the lower part of the unit. The upper part is made of fine-grained sandstone with a fossiliferous limestone at the top. The combined thickness of the cliff-forming gypsum and slope-forming sandstones is 16 m.

The uppermost Winsor Member consists of light red to pale orange to light gray sandstone. These low slope-forming sandstones are approximately 65 m thick in the area immediately north of Carmel Junction.

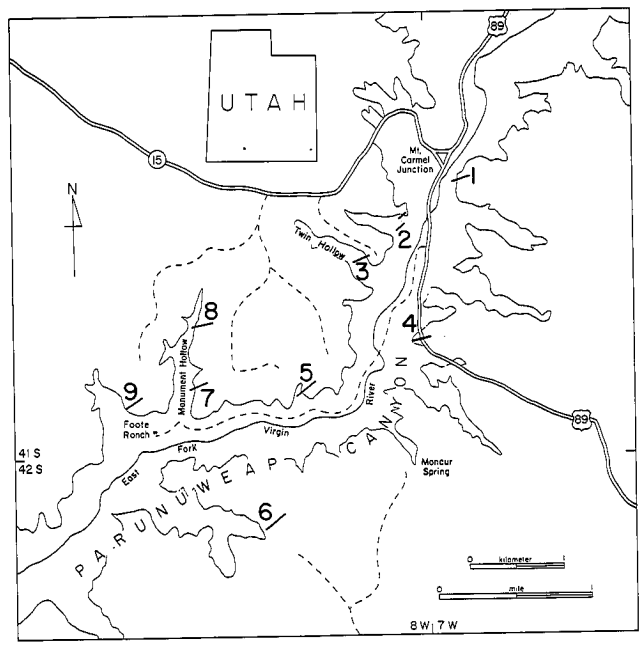


FIGURE 1.–Index map of the Carmel Junction area, showing locations of the measured sections.

*A thesis presented to the Department of Geology, Brigham Young University, in partial fulfillment of the requirements for the degree Master of Science, April 1981. Thesis chairman: J. Keith Rigby.

### Location

Measured sections of the study are located immediately to the south and southwest of Carmel Junction in west central Kane County, Utah (fig. 1). Sections of the limestone member of the Carmel Formation were measured in Parunuweap Canyon and in minor tributaries to the east fork of the Virgin River. Sections 1 and 2 are adjacent to U.S. 89. Sections 3 through 9 are accessible via logging roads and by walking to the rim of Parunuweap Canyon. All the sections are in Townships 41 and 42 South and Ranges 7 and 8 West (fig. 4).

### Methods of Study and Nomenclature

Nine stratigraphic sections of the limestone member of the Carmel Formation were measured with a 15-m fiberglass tape and Brunton compass or with a 1.5-m Jacob staff. Thicknesses of the sections range from 62 m to 80 m. Each section was subdivided into units on the basis of lithology, color, composition, bedding, bioclasts, and sedimentary structures. Paleocurrent directions were determined with the use of a Brunton compass on structures, such as cross-bedding, ripple marks, and drag marks. Samples were collected from each distinct unit. On one particularly promising weathered slope, approximately 15 kg of unconsolidated fossiliferous material were collected for screening and paleontologic study.

Thin sections of each major lithology were examined under binocular and petrographic microscopes to determine fabric and composition. The unconsolidated material was washed and screened and then examined for microfossils under a binocular microscope. Alizarin Red S and potassium ferricyanide stains (Friedman 1959) were used to determine calcite and dolomite content. Samples from lithofacies E were weighed and then dissolved in dilute HCl for clay-carbonate ratios. The carbonate nomenclature proposed by Dunham (1962), which classifies rocks on the basis of texture, was used.

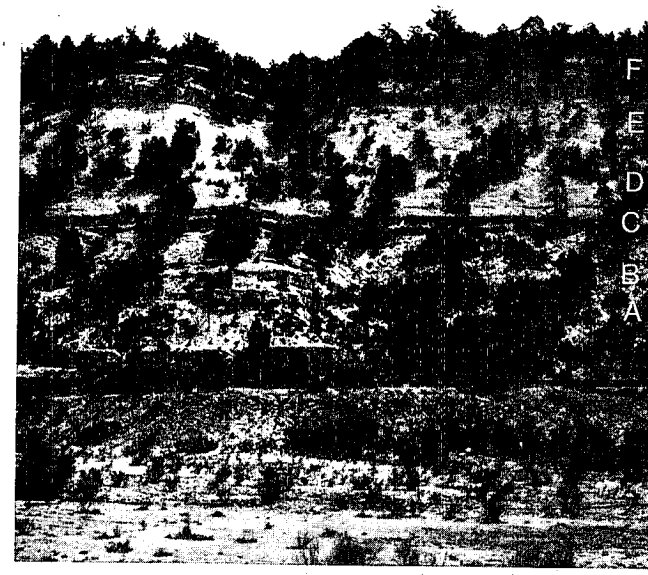


FIGURE 3.–View of Carmel Limestone Member, showing lithofacies A through F at section 1.

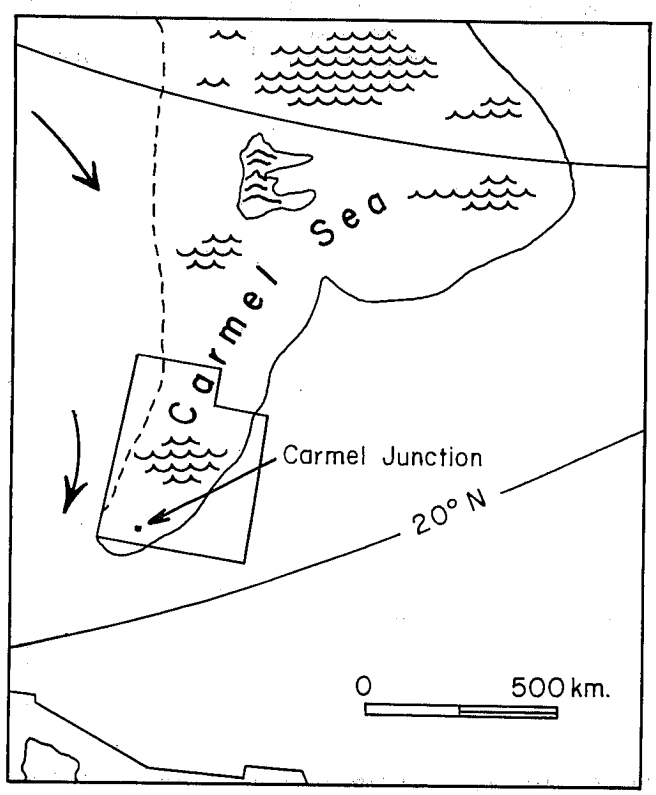


FIGURE 2.–Paleogeographic map of the western United States showing extent of the Carmel Sea into southern Utah (modified from Lowrey 1976). Arrows indicate wind directions (Bigarella 1972, p. 56).

### Previous Work

Powell (1875) originally noted the Carmel Formation as a distinct unit above the Vermilion Cliffs. The name *Carmel Formation* was proposed for this unit in 1924 at a joint conference that involved H. E. Gregory, R. C. Moore, and J. B. Reeside (Wilmarth 1938, p. 351). The type section selected by them is that described by Gilbert near the town of Mount Carmel, Utah.

The Carmel Formation has been studied as a gross unit by many workers, but no published detailed studies are available on the Carmel Junction area. Early reconnaissance work on the Carmel Formation was published by Gilluly and Reeside (1928) and by Baker, Dane and Reeside (1936). Gregory (1950) carried out regional studies in southern Utah and published papers that contained significant broad data on the Carmel Formation. Imlay (1952, 1957, 1964, 1967) worked out a general time-stratigraphic subdivision of Jurassic formations of the western interior of the United States, and discussed correlation of the Carmel Formation with other equivalent rocks.

McKee and others (1956), Wright and Dickey (1963, 1978, 1979), and Stokes and Heylum (1965) conducted regional studies of the San Rafael group in the Paunsaugunt and Kaiparowits Plateaus and measured sections of the Carmel Formation in south central Utah. Cashion (1967) produced geologic maps of part of Kane County, including outcrops of the Carmel Formation. Thompson and Stokes (1970) studied the San Rafael Group to the north and east of the study area. More recently paleoenvironmental studies were carried out by Lowrey (1976) in the Sheep Creek Gap area on the north flank of the Uinta Mountains, and by Bagshaw (1977) on the western slope of the San Rafael Swell. Peterson and Pipiringos (1979) published data on the Middle Jurassic formations of southern Utah and northern Arizona. Gessaman and Voorhees (1980) also have recently published regional data on the Carmel Formation.

Acknowledgments

The writer acknowledges the assistance and encouragement of Dr. J. K. Rigby, thesis chairman. The helpful suggestions of Dr. H. J. Bissell with environmental interpretation, thin section analysis, and critical review of this thesis are also appreciated. My father, Jim Taylor, and Dave Jenkins, a fellow student, helped with the fieldwork and are gratefully acknowledged. Sincere thanks are expressed for the kindness of Leonard H. Foote, M.D., who allowed me to stay at his ranch while the field study was being made. The assistance of Richard Boardman and Bill Oliver of the United States National Museum and John Wray of Marathon Oil Company with fossil identification is acknowledged. I thank my parents for the help and support they gave me while the study was being made. Special thanks are given to my wife, Michelle, for her constant encouragement and help with the fieldwork and for typing the manuscript. Financial assistance was provided by Amoco Production Company and by Brigham Young University Department of Geology.

## GEOMETRY AND PETROLOGY OF LITHOFACIES

The basal limestone member of the Carmel Formation near Carmel Junction is divided into six lithofacies (A through F in ascending order) on the basis of outcrop appearance, lithology, and thin section analysis (fig. 4). Carbonates are the dominant rocks in the area, but clastic rocks also occur in the member. Brown to grayish brown siltstones interfinger with lithofacies B, C, and F. These poorly exposed units form slope zones between the ledgy, cliff-forming dolomite and limestone units. Eight subfacies are also differentiated to facilitate description and interpretation. Figure 4 shows thicknesses and correlation of the lithofacies.

### Lithofacies A

The lower clastic lithofacies A extends upward from the contact of the Carmel Limestone on the White Throne Member of the Temple Cap Sandstone to the lowest occurrence of dolomitic limestones of carbonate lithofacies B (fig. 3). These lower clastic rocks form one of the more consistent units throughout the area. They range from 3.5 m thick in sections 1 and 2 to more than 5 m thick in sections 5 and 6. That variation may be related to poor exposures, which make finding a consistent base difficult.

Although the exact lower contact of the unit is variable throughout the study area, it is marked by a distinct change in erosional profile from the cliff-forming White Throne Member of the Temple Cap Sandstone up to the basal slope-forming clastic unit of the Carmel Formation. This lower contact has been termed the J-2 unconformity by Peterson and Pipiringos (1979). The upper contact of lithofacies A is also well marked by an erosional change from the slope-forming sandstone and siltstone of lithofacies A to the overlying cliff-forming, grayish pink, dolomitic siltstone of lithofacies B (fig. 4).

Mineralogically, the lower clastic lithofacies consists mainly of quartz, with less than 20 percent clay minerals, calcite, biotite, and other terrigenous clastic fragments.

Sandstone predominates in lithofacies A, with less siltstone and shale. Sandstone beds are massive, and the finer clastic units are thinly bedded. Subangular, moderately well sorted quartz grains characterize the greenish gray sandstone and are in a matrix of clay minerals. Rocks of lithofacies A are not calcareous, except in the upper 20 cm where the pale red or greenish gray mottled sandstone is calcareous. Biotite grains are approximately 0.4 mm in diameter in a 25-cm bed in the middle lithofacies A in sections 1 and 2, where the total unit is well exposed. The hexagonal biotite grains are not altered and have sharp clear corners indicating that transport was minimal and that these minerals may have had a nearby source or were parts of an airfall tuff.

### Lithofacies B

Lithofacies B consists, for the most part, of dolomitic mudstone and siltstone and extends upward from the slope-forming clastic lithofacies to the lowest occurrence of skeletal and oolitic limestone of lithofacies C. The lithofacies varies from 7 m thick in section 1 to nearly 15 m thick in section 3 (fig. 3) and shows westward and southwestward thickening.

The lower contact of the lithofacies is marked by a break in erosional profile, as well as a lithologic break, from the slope-forming, pale purplish red and greenish gray, mottled sandstone of clastic lithofacies A to the cliff-forming, light grayish pink, dolomitic siltstone of lithofacies B. The upper contact is marked by the lowest occurrence of skeletal-oolitic limestone (fig. 4).

Lithofacies B consists of approximately 70 percent dolomite. Quartz, anhydrite, and fine terrigenous clastic fragments make up the rest of the rocks.

Lithofacies B is divided into four subfacies: they are from the base up, a siltstone, a dolomicrite, a stromatolitic boundstone, and an evaporitic dolomicrite subfacies.

#### *Siltstone Subfacies*

The siltstone subfacies is a laterally continuous unit throughout the study area and makes up nearly 5 percent of the lithofacies thickness. Siltstone occurs at the base of lithofacies B and grades upward into the dolomicrite subfacies. In outcrop it appears as a grayish pink, cliff-forming, thinly laminated sequence.

Quartz grains and minor dark ferromagnesian minerals are cemented by dolomicrite and occur in the thin irregular laminae that characterize this subfacies (fig. 5).

#### *Dolomicrite Subfacies*

The dolomicrite subfacies makes up nearly 90 percent of the thickness of lithofacies B. These rocks occur as cliffs to ledgy slopes up to 8 m thick. The subfacies is characterized by thinly laminated dolomicrite, massive dolomicrite, and cryptalgal dolomicrite.

The thinly laminated dolomicrite, as the name implies, has laminae up to 6 mm thick. These rocks contain approximately 10 to 20 percent angular quartz grains. Fine micritic dolomite and fine-grained terrigenous debris make up the remainder of the matrix (fig. 6).

The massive dolomicrite is dense, is commonly porcelaneous, lacks fine stratification, and is generally featureless. It forms flaggy-weathering, ledgy cliffs.

Figure 7 shows cryptalgal bedding in a dolomicrite unit from section 7, unit 13. Such bedding is interpreted to result from thin discontinuous algal films.

Organic activity must have been limited during deposition of this lithofacies. No whole fossils were found, and bedding is generally undisturbed.

#### *Stromatolitic Boundstone Subfacies*

The stromatolitic boundstone subfacies comprises less than 5 percent of lithofacies B in sections where it is found. These

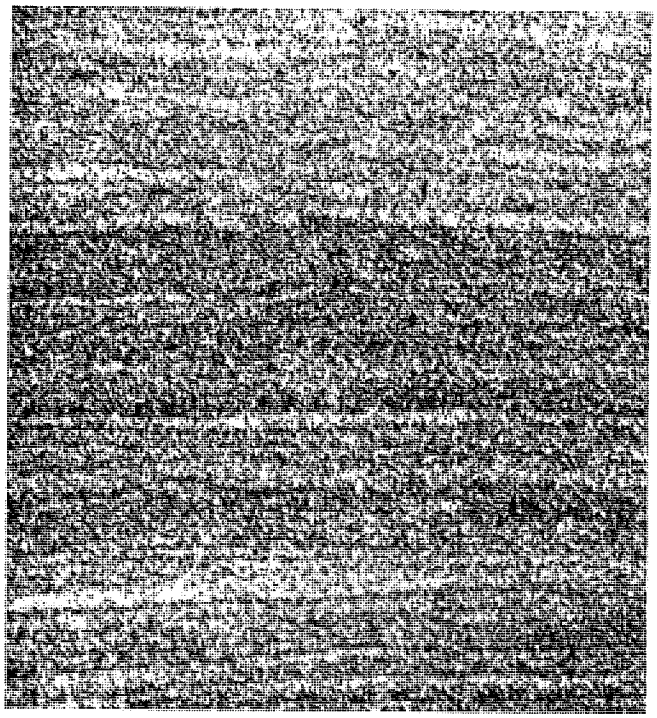

FIGURE 5.–Photomicrograph of dolomitic siltstone subfacies showing thin laminae of fine quartz grains and dolomicrite from section 1, unit 8, X5.5.

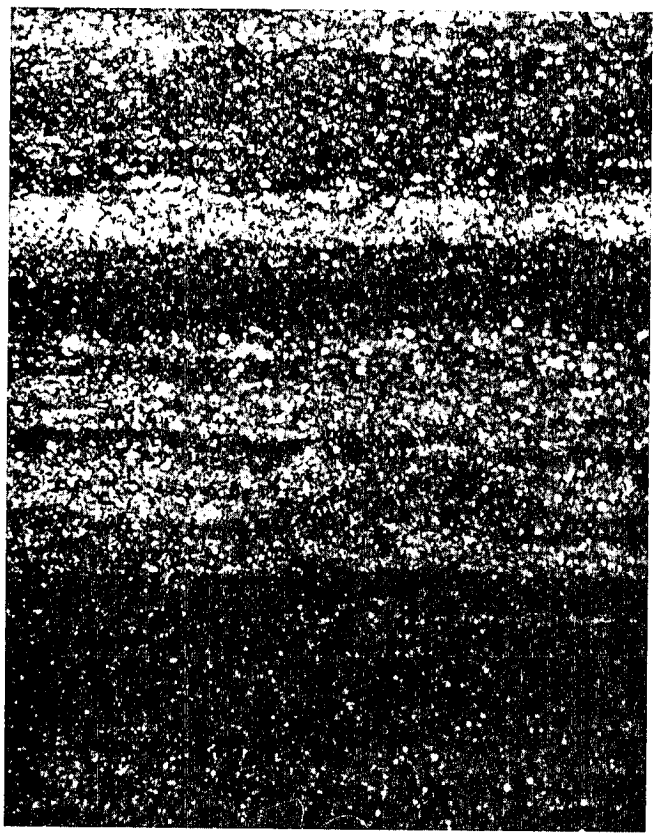

FIGURE 6.–Photomicrograph of thinly bedded dolomicrite showing thin laminae with silt-sized quartz grains scattered in matrix from section 1, unit 9, X7.85.

rocks are 0.25 m thick at their thickest in section 1 and are normally limited to the lower half of the lithofacies.

Petrographically, the subfacies is characterized by dolomicrite with an irregular fenestral fabric which contains fine, silt-sized quartz in the matrix. Individual fenestrae are both oval (birdseye) and tabular with cavities up to 6 mm long. Most fenestrae are 2 to 3 mm long and are characteristically filled with anhydrite.

Thin sections show iron-stained filamentous laminae. The filaments may represent remains of the original trapping algae. The stromatolites consist of crinkly to undulatory, continuous laminae and are probably the LLH variety of Logan and others (1964, p. 77; fig. 8).

*Evaporitic Dolomicrite Subfacies*

In section 2, a 3.5-m-thick unit of dolomicrite contains two beds of nodular anhydrite, each approximately 0.3 m thick–the best exposure of the subfacies in the eastern sections. All the western sections have well-exposed beds of the evaporite subfacies (fig. 4).

FIGURE 7.–Cryptalgal bedding in the dolomicrite subfacies of section 7, unit 13.

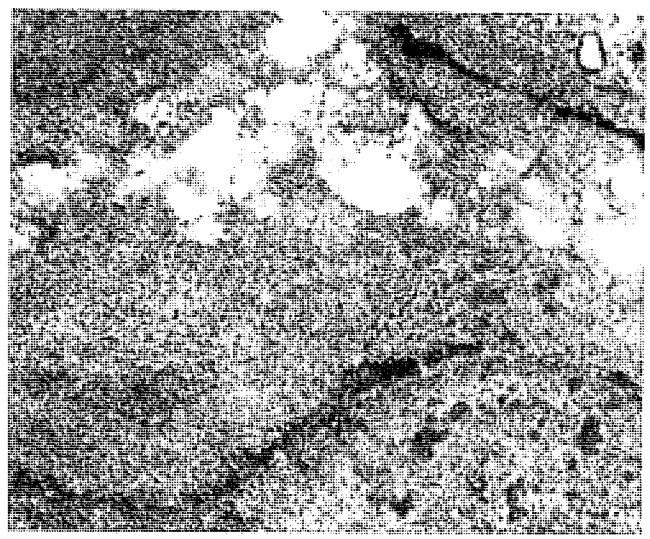

FIGURE 8.–Photomicrograph of stromatolitic boundstone in section 1, unit 11. Thin irregular bedding may represent original trapping algae. Birdseye fenestrae are filled with anhydrite, section 1, unit 11, X3.8.

The subfacies is characterized by nodules of anhydrite up to 1 cm thick in dolomicrite. They are typically ovate but may occur as flattened broad lenses that have a bedded appearance. A thin rind of reddish yellow dolomicrite surrounds the anhydrite as a lacy layer and probably represents excluded sediment that was pushed aside as the anhydrite crystals grew (fig. 9).

No trace fossils or whole fossils were observed in the subfacies, and sedimentary structures are limited to a crinkly chicken-wire-like fabric resulting from the dolomicrite rinds around the nodules.

### Lithofacies C

Lithofacies C includes the skeletal limestones in the area and occurs as three major lenses. The lenses are thickest in sections 2, 5, and 7, and are thinner throughout the rest of the area (fig. 4). The base of lithofacies C is marked by the distinct lithologic break from dolomicrite upward to skeletal limestone. The contact with overlying lithofacies D is the most distinct contact in the Carmel section. It is an abrupt lithologic break from the cliff-forming skeletal limestone of lithofacies C to the broad, low-slope-forming shale of lithofacies D (fig. 3).

Rocks of lithofacies C are 95 percent calcite with minor amounts of iron oxides and clay or other terrigenous clastic material.

The two distinct subfacies recognized in the lithofacies are a lower oolite to skeletal packstone or grainstone subfacies and upper bivalve wackestone subfacies.

#### *Oolite Skeletal Packstone and Grainstone Subfacies*

Oolite skeletal packstone and grainstone make up the lower 75 to 85 percent of the lithofacies and weather to cliffs and ledges. These yellowish gray rocks usually exhibit undulatory bedding at the base but cross-bedding at the top, with cross-bed sets up to 25 cm thick (fig. 10).

Rocks of the subfacies consist mainly of oolites, intraclasts, and coated bioclasts of bivalves, echinoids, crinoids, algae, and bryozoans (fig. 11) in a micrite to spar matrix. Sorting is poor, and the allochems are broken and abraded (fig. 12). Grainstones consist mostly of echinoderm fragments, indicating a higher-energy environment (fig. 13). Allochems of bivalve and echinoderm material are common (figs. 14 and 15). One regular echinoid corona was found intact in unit 13 of section 6 (fig. 16A). Bivalve fragments have been partially recrystallized into spar. Oolites also show recrystallization to a degree. Interstitial matrix is mostly spar or pseudospar, which has been recrystallized from the original micrite (fig. 12).

FIGURE 10.–Cross-bedded oolite-skeletal packstone in section 3, unit 11.

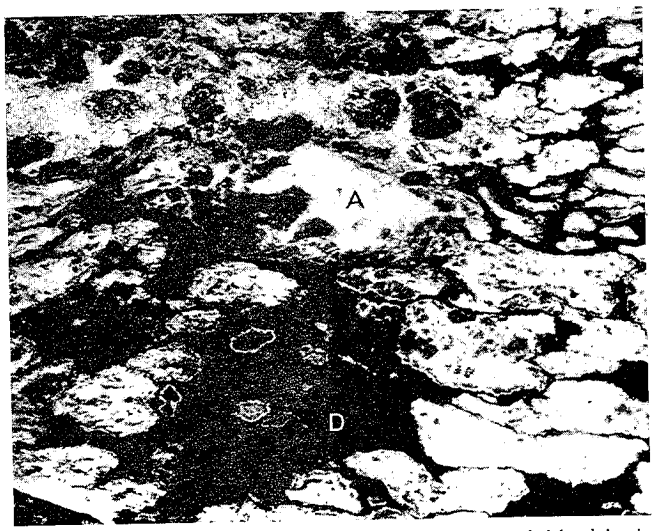


FIGURE 9.–Photomicrograph of nodular anhydrite (A) surrounded by dolomicrite (D) from section 6, unit 6, X3.8.

#### *Bivalve Wackestone Subfacies*

Rocks of this subfacies make up the remaining 25 percent of lithofacies C. They are light olive gray and form a broad slope zone above the cliffs of the oolite skeletal packstone subfacies. Thickness of the subfacies varies from 1 m in section 8 to nearly 2 m in section 6, and in some of the sections it is covered by float, as for example in sections 2, 3, 4, and 5, in the Carmel Junction area (fig. 4). Partially recrystallized bivalve fragments, most less than 1 cm across, occur as floating clasts in the micrite matrix (fig. 17). Less common fragments of *Pentacrinus,* as well as echinoderms, bryozoans, bivalves, and clay

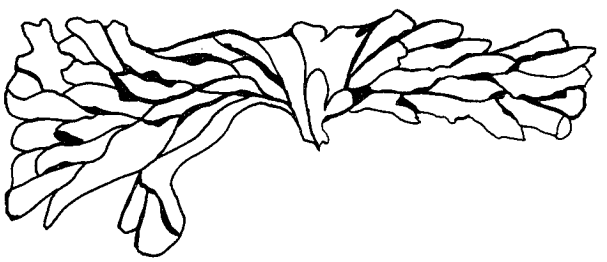

FIGURE 11.–Drawing of possible bryozoan colony of figure 16F, X20.

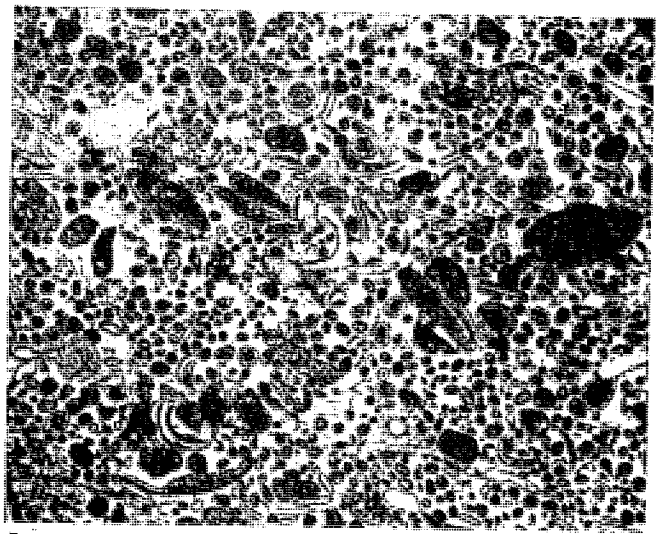

FIGURE 12.–Photomicrograph of oolite-skeletal packstone of unit 19, section 1, showing oolites, bivalve, and echinoderm material floating in a spar matrix, X4.

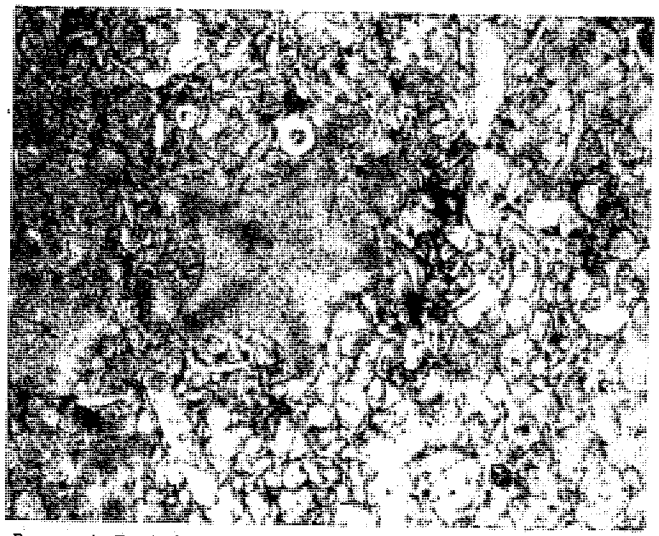

FIGURE 14.–Encrinal grainstone showing *Pentacrinus* columnal and other echinoderm fragments, peel X8.

intraclasts have also been observed in the matrix (fig. 18). The subfacies has a massive appearance, probably due to disruption or destruction of bedding by bioturbation. Vertical *Skolithos* burrows, up to 3 mm in diameter, are common in the subfacies. Whole fossils of bivalves, bryozoan colonies, and a possible coelenterate fragment were collected from weathered debris of the subfacies in section 1, unit 21, and section 7, unit 23 (fig. 4).

### Lithofacies D

Grayish green to purplish red shale of lithofacies D comprises the lower part of the middle prominent slope within outcrops of the limestone member of the Carmel Formation (fig. 3). The basal contact is placed at the top of the bivalve wackestone of lithofacies C. Lithofacies D extends upward to the lowest argillaceous limestone mudstone of lithofacies E (fig. 19). Placement of the top is somewhat arbitrary because it is invariably covered by float and requires trenching for precise limitation, except in section 4 where the boundary is distinct.

Clay minerals make up 95 percent of these rocks. Calcite and quartz make up the remaining 5 percent.

Lithofacies D, although poorly exposed in every section except section 4, can be divided into a lower and an upper shale sequence, separated by a medial ledge-forming argillaceous mudstone. Lower and upper shales are similar in color and composition. Both are grayish green to reddish purple and contain fine intermixed silty mud. The medial argillaceous mudstone is thinly laminated and forms a 2-m-thick ledge between the two slope-forming shale units (fig. 19).

Whole fossils and trace fossils are virtually absent in the shale.

### Lithofacies E

Olive gray argillaceous limestones of lithofacies E weather to the upper platy part of the slope of the Carmel Limestone Member (fig. 3). Lithofacies E is the most uniform of all lith-

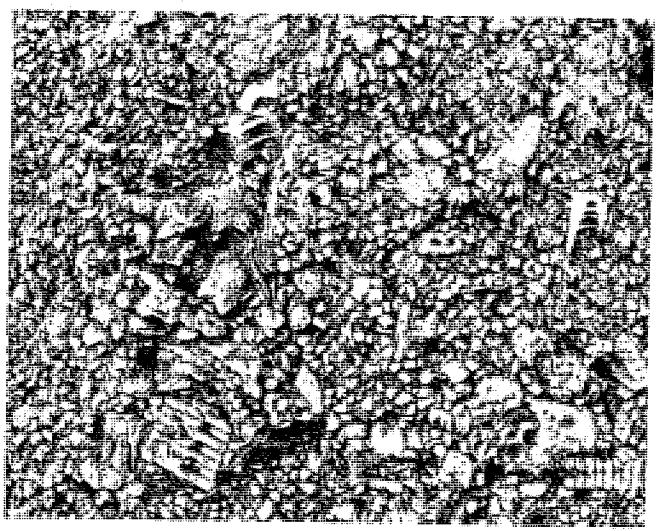

FIGURE 13.–Weathered surface of packstone from section 7, unit 22, showing *Pentacrinus* and bivalve and echinoderm detritus, X1.6.

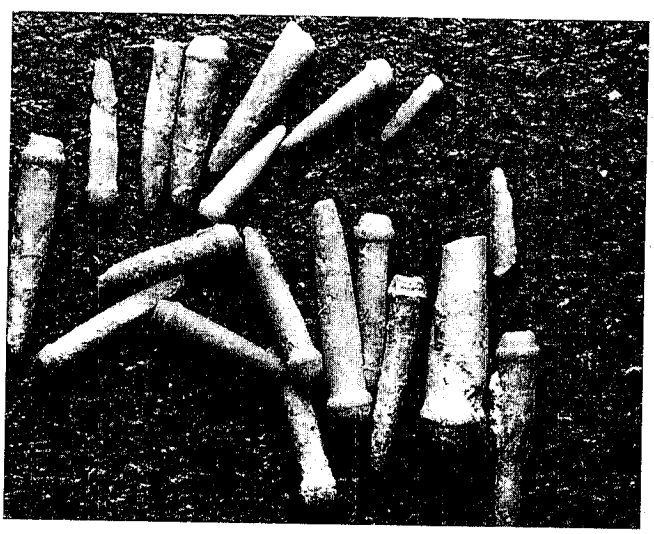

FIGURE 15.–Echinoid spines from section 7, unit 23, BYU 2868, X8.

ofacies in the study area, for no lateral variation of composition or texture was observed. The lower boundary is difficult to define precisely because it is covered by float, except in the excellent roadcut exposures of section 4. For this reason the boundary is placed at the lowest outcrops of these limestone mudstones (fig. 19). The lower facies boundary also can be placed at the level where the slope angle increases markedly. Upper beds of the lithofacies interfinger with peloidal grainstones of lithofacies F; accordingly, this boundary is more or less transitional. Thickness of lithofacies E ranges from 18 m in eastern sections, to 22 m in western sections (fig. 4). Rocks of lithofacies E consist of approximately 70 percent calcite and 30 percent argillaceous material.

The lithofacies is characterized by very thin graded laminations, as shown in figure 20A. Ripple marks are apparent where weathering has etched them into relief on the rocks (fig. 20B). Whole fossils and trace fossils are absent in lithofacies E.

### Lithofacies F

Prominent ledges and cliffs at the top of the limestone member of the Carmel Formation are held up by lithofacies F (fig. 3). It extends upward from the lowest occurrence of predominantly yellowish gray peloidal grainstones to the base of the silty redbeds of the banded member of the Carmel Formation (fig. 19). Thickness of lithofacies F in the measured section ranges from less than 5 m in section 9 to 14 m in section

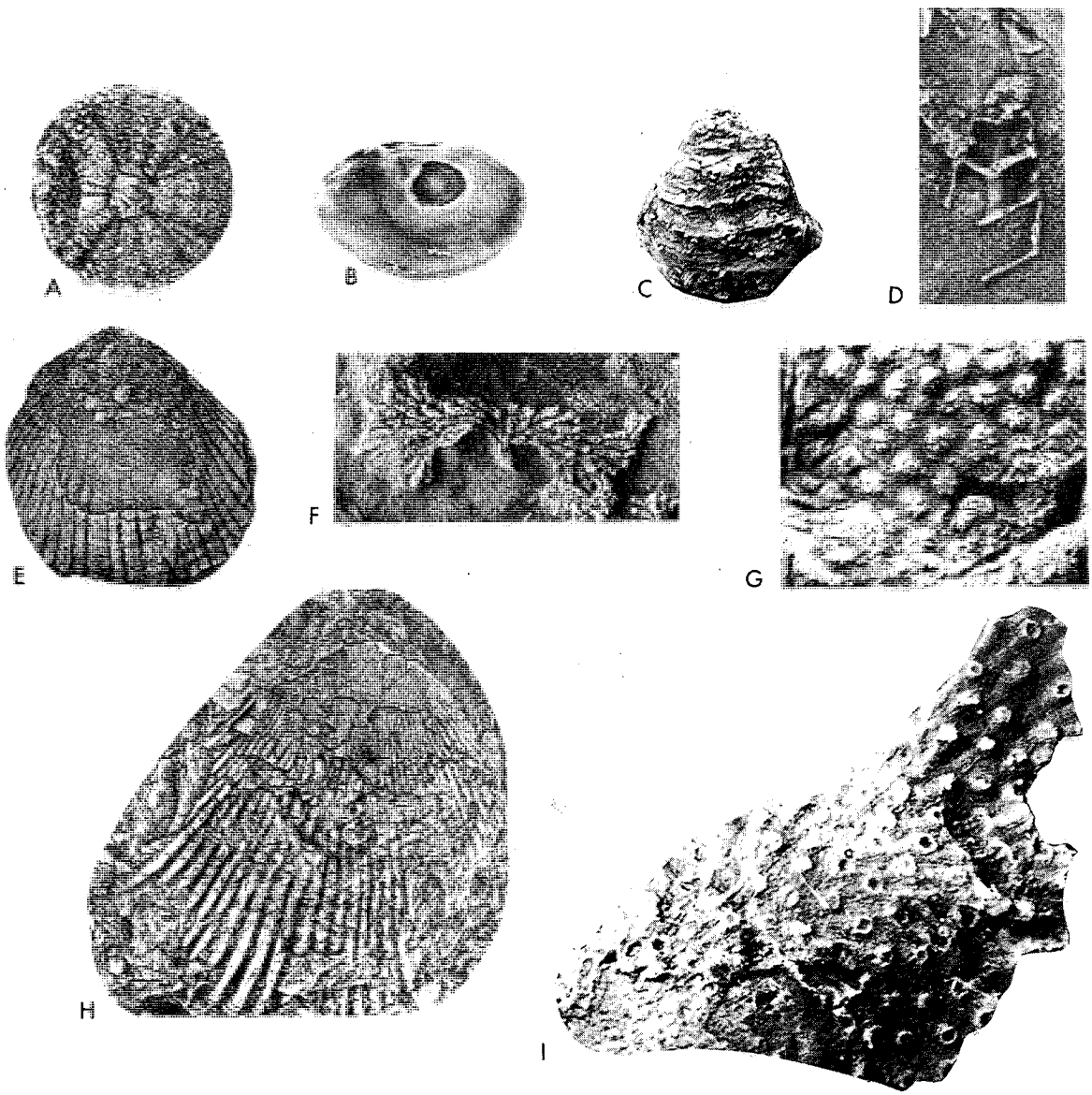


FIGURE 16A.–Regular echinoid, *Diademopis* Desar, from section 6, unit 13, BYU 2869, X2. B.–*Ostrea (Liostrea) strigulecula* White from section 7, unit 3, BYU 2867, X2. C.–*Gryphaea* valve from section 1, unit 21, BYU 2866, X2. D.–*Cossmannea imlayi* Sohl from section 5, unit 18, BYU 2870, X2. E.–Right valve of *Lima (Plagiostoma) zonia* Imlay, from section 7, unit 23, BYU 2865, X1. F.–Possible cyclostome bryozoan colony encrusting an *Ostrea* shell, X10. G.–Coelenterate ? colony from section 8, unit 11, X2. H.–Left valve of *Lima (Plagiostoma) occidentalis* Hall and Whitfield, from wackestone in the Moncur Spring area, BYU 2862, X1. I.–*Mesenteripora* Blainville encrusting an *Ostrea* shell, BYU 2863, X10.

FIGURE 17.–Photomicrograph of wackestone subfacies of section 1, unit 21, showing bivalve fragments floating in carbonate mud, X4.

1 (fig. 4). In sections 5 through 9, the top of lithofacies F is eroded so that total thicknesses of these rocks are not known, for the banded member of the Carmel Formation has been stripped back by slope retreat.

Rocks of lithofacies F consist of over 90 percent calcite, with the remainder of fine quartz grains, limonite, and trace amounts of anhydrite. The two subfacies defined in lithofacies F are two of peloidal grainstone and a middle stromatolitic boundstone.

*Peloidal Grainstone Subfacies*

The peloidal grainstone subfacies comprises up to 80 percent of lithofacies F in all sections. The subfacies is typically massively bedded, with prominent cliffs up to 6 m high, at both the base and top of the lithofacies (fig. 3). A 2-m siltstone slope zone generally separates the upper and lower cliffs.

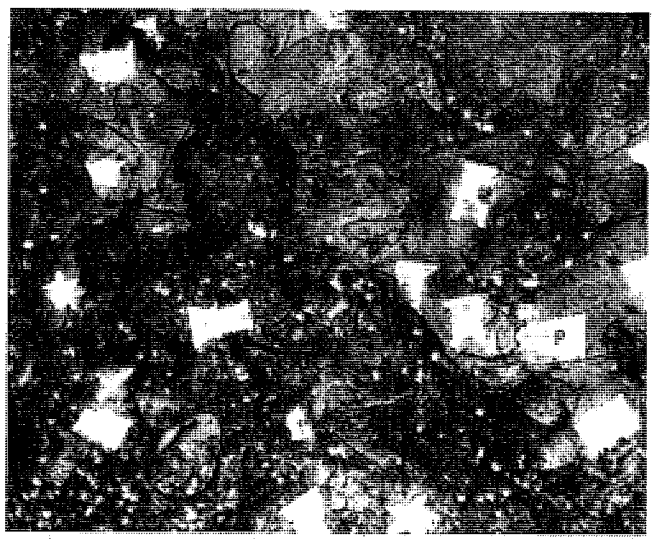


FIGURE 18.–Wackestone subfacies from Moncur Spring area, showing *Pentacrinus* columnals (P), as well as echinoderm, bryozoan, and bivalve fragments in carbonate mud matrix, polished slab, X1.6.

Yellowish gray limestone of the subfacies is characterized by well-sorted spherical to oval peloids approximately 0.1 mm in diameter. The matrix consists of recrystallized micrite (fig. 21).

Bivalve coquinas are found, with few exceptions, in portions of the upper cliff of the subfacies. The valves are disarticulated in the 2-cm- to 3-cm-thick beds (fig. 22). High-spired gastropods were collected from unit 18 of section 5 of the subfacies. A petroliferous odor is released when these peloidal grainstones are broken.

Vugs were observed in most outcrops of the subfacies (fig. 4). These openings probably were produced where calcite has been leached out. Current-produced sedimentary structures were observed in rocks at the top of the subfacies and in thin section (fig. 21). Figure 23 shows ripple marks, with the head of the hammer pointing toward the northwest in the direction of current flow. Compass readings from several areas indicate currents from the northwest to the northeast.

*Stromatolitic Boundstone Subfacies*

The stromatolitic boundstone of lithofacies F comprises less than 5 percent of the lithofacies. Unlike the stromatolitic boundstone near the base of the formation in lithofacies B, these younger boundstones are made of quartz grains in fine carbonate mud. These rocks usually crop out at the top of the lower cliff of the peloidal grainstone subfacies. The thickness accumulation of the subfacies occurs in section 2 where these rocks are nearly 1 m thick (fig. 4). In outcrop they appear as low ledges that weather in a crumbly fashion.

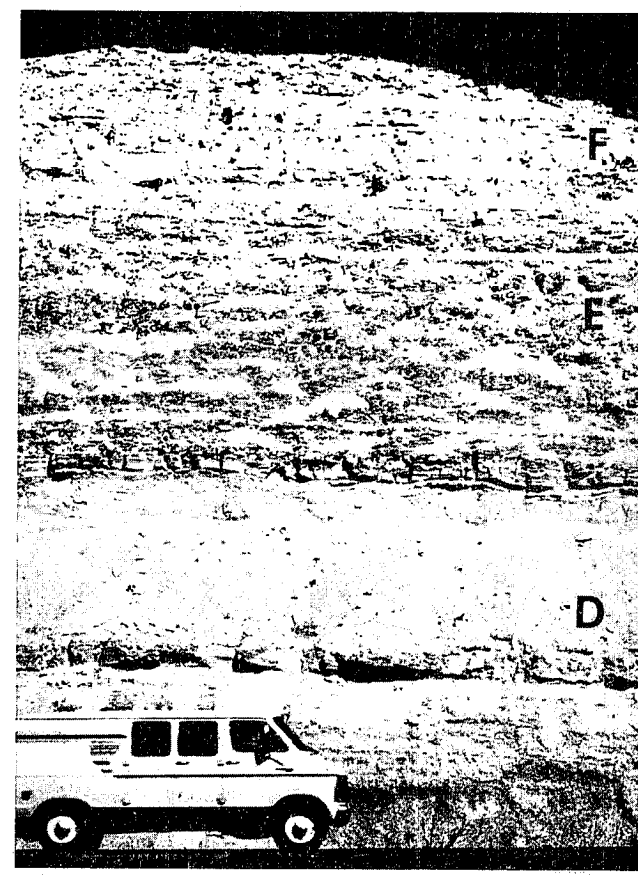


FIGURE 19.–Units of lithofacies D, E, and F exposed in roadcut of section 4.

Relict fenestral fabric has left vugs that produce up to 20 percent porosity and give a "spongy" appearance to the weathered rock.

## CORRELATION

The lower limestone member of the Carmel Formation correlates with Piper-Nesson-age rocks of Peterson (1972, p. 177). These rocks represent marine deposition during the second regional transgression of Jurassic seas from the Arctic region into the Rocky Mountain and Colorado Plateau Provinces of North America. Rocks of this age are predominantly carbonates throughout the Utah-Idaho trough, where they are thickest (Imlay 1967, p. 2). This calcareous sequence changes eastward and southeastward to redbeds in central Wyoming and eastern Utah.

The limestone member is approximately correlative with rocks in the Upper Sawtooth and Middle Piper interval in Montana and northern Wyoming. The Rich Member of the Twin Creek Limestone in southwestern Wyoming is most nearly correlative with the Carmel Formation limestone member.

Imlay (1967, p. 33) concludes that, because the limestone member is poorly fossiliferous in southern Utah, it may correlate with the Sliderock Member of the Twin Creek Limestone in northeastern Utah. It is generally accepted that the middle Twelvemile Canyon Member of the Arapien Shale in central Utah correlates with the Carmel Formation limestone member in southern Utah (Imlay 1967, p. 20).

## PALEONTOLOGY

Fossils from the limestone member of the Carmel Formation in the study area represent a restricted mollusk fauna, dominated by bivalves. Echinoderms, although limited, are also represented in collections from the area. Preservation is generally poor, inasmuch as most fossils were transported and abraded and many show partial recrystallization. All identifiable body fossils collected during the study came from lithofacies C and F.

Bivalves are abundant throughout the oolite skeletal packstone and grainstone subfacies of lithofacies C and occur in coquinas of lithofacies F. Most bivalve materials have undergone partial recrystallization; however, identification of larger fragments was made possible by comparison to whole fossils such as those in Imlay (1967, plates 1–4).

*Ostrea* and related oysters are probably the most common bivalves found in the area (fig. 16B). They occur mostly in packstones and wackestones of lithofacies C. Broken *Ostrea* shells make up most of the bivalve allochems observed in thin section (fig. 17). One small, but nearly complete, *Gryphaea* valve was found in weathered rubble from the wackestones of lithofacies C, in section 1, unit 21. Imlay (1967) reported that *Gryphaea* had not been found, to that date, from the Carmel Formation or correlative rocks south of Thistle, Utah (fig. 16C).

The *Lima* suite of bivalves is restricted to the wackestone subfacies of lithofacies C. *Lima (Plagiostoma) occidentalis* Hall and Whitfield was found on weathered surfaces of the bivalve wackestone subfacies in the Moncur Spring area (fig. 16H). Whole *Lima (Plagiostoma) zonia* Imlay valves are commonly found in weathered wackestone rubble (fig. 16E).

Molds of small *Camptonectes stigius* White were also collected from the rubble of the bivalve wackestone subfacies in section 1, unit 21. *Camptonectes* makes up the bivalve coquinas of lithofacies F (fig. 22).

Section 5, unit 18, yielded the only gastropods found in the study area. Figure 16D shows a longitudinal cross section of a high-spired *Cossmannea imlayi* Sohl on the weathered surface of a sample of the peloidal grainstone subfacies of lithofacies F.

Echinoderm fossils are restricted to both subfacies of lithofacies C. Whole, as well as broken, echinoid spines and *Pentacrinus* columnals make up approximately 30 percent of the allochems in these rocks (figs. 12, 13). No *Pentacrinus* calices were found. A small, well-preserved, regular echinoid *Diademopis* Desar (Moore 1966, p. 357–58) was collected, however, from section 6, unit 13 in lithofacies B (fig. 16A).

Cyclostome bryozoans were discovered in thin sections and as whole fossils in samples from both subfacies of lithofacies C. Figure 24 shows colonies of unilaminate bryozoans in thin section parallel to bedding in packstone from section 4, unit 11. Figure 16I shows the convoluted broad expansion of zooaria of probably the same cyclostome bryozoan encrusting a bivalve shell. Figure 11 is a drawing of possible bryozoan colony of figure 16F. Richard Boardman of the United States National Museum identified the bryozoan in figure 16I as a form of *Mesenteripora* Blainville (Moore 1953, p. 50), which is usually restricted to the Bathonian of northern Europe.

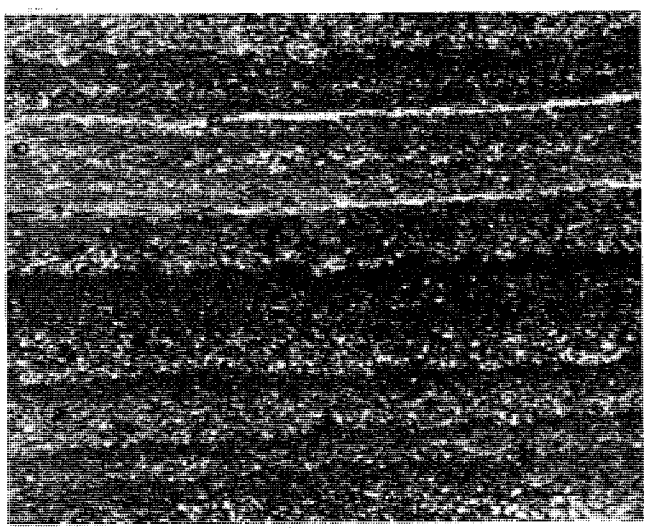

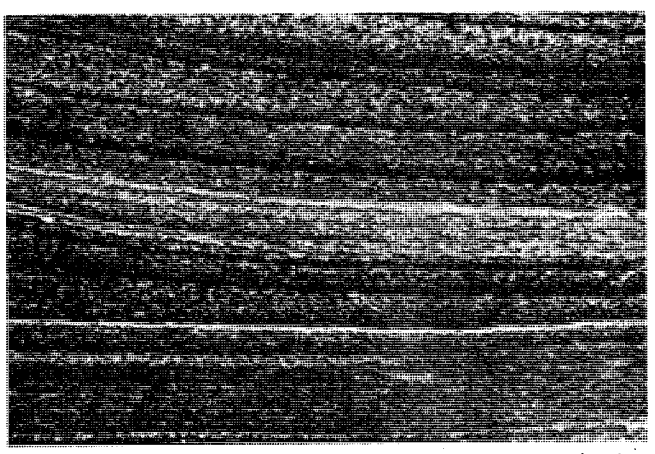

FIGURE 20A.–Photomicrographs of argillaceous mudstone of section 5, showing (A) thin laminae of graded bedding, suggesting storm surges in repeated cycles, X8 B.–Micro-cross-bedding of lithofacies E, X4.

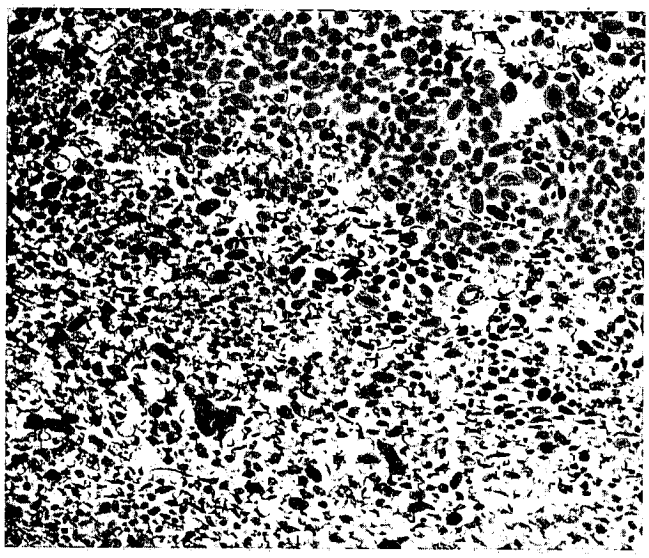

FIGURE 21.–Photomicrograph of peloidal grainstone of lithofacies F in section 4, unit 18, showing current laminated peloids, X10.

A possible coelenterate ? was collected from lithofacies C in section 8, unit 11 (fig. 16G).

### Ichnology

Trace fossils are relatively uncommon in the limestone member of the Carmel Formation. Vertical *Skolithos* burrows occur in beds of the bivalve wackestone subfacies. Seilacher (1967) interpreted *Skolithos* to indicate shallow marine to intertidal deposition. Pascichnid grazing trails were observed in the upper part of lithofacies F in the type section of the Carmel Limestone Member at Carmel Junction, but other facies lack trace fossils.

## DIAGENESIS

Diagenesis has played an important role in preservation and destruction of original fabrics of the Carmel Formation limestone member. Recrystallization of anhydrite and replacement after gypsum and dolomitization have materially affected textures in rocks of lithofacies B. Neomorphic recrystallization of matrix and allochems is common in rocks of lithofacies C and F. Leaching of calcite has left voids in rocks in lithofacies F.

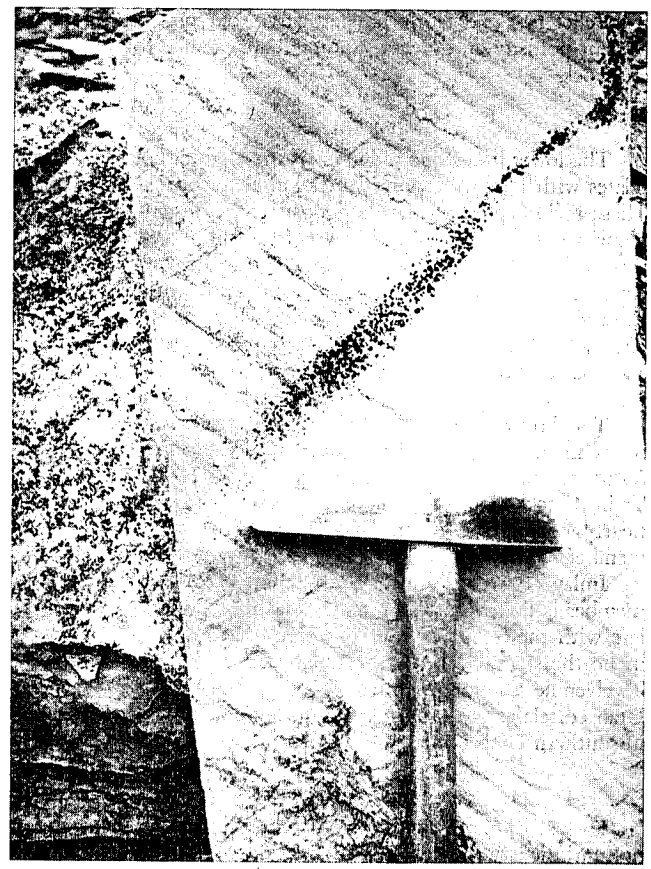

FIGURE 23.–Ripple marks in dolomicrite from section 3, unit 8.

### Recrystallization

Nodular anhydrite after gypsum is found in several units of lithofacies B and to a lesser degree in lithofacies F. These anhydrite nodules range from ovate to flattened masses that give the

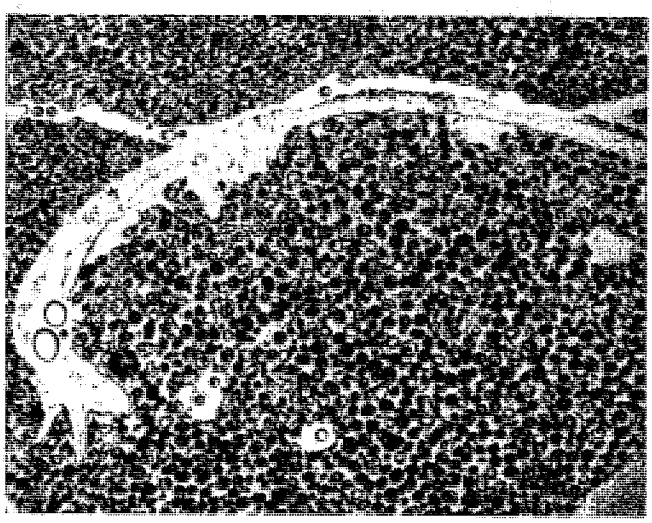

FIGURE 22.–Photomicrograph of peloidal grainstone of section 5, unit 21, showing recrystallized bivalve shell surrounded by peloids, X8.


FIGURE 24.–Photomicrograph of packstone from section 4, unit 11, showing colonies of *Mesenteripora* (B), bivalve (b), and echinoderm material, X4.

appearance of bedded anhydrite. Kerr and Thomson (1963) studied Laguna Madre coastal sediments of south Texas and compared their findings with observations on Permian shelf sediments of west Texas. Crystal aggregates of gypsum from Laguna Madre are analogous to some Permian anhydrite nodules. Difference in internal crystal fabric of the Recent gypsum vs. fine, felted blade and fibrous masses of Permian anhydrite probably result from crystal reorganization upon dehydration of gypsum during conversion to anhydrite after burial. Expansive crystal growth within unconsolidated sediments may result in physical disruption of layered sediments. Such growth also explains exclusion and shouldering aside of the host sediment in the Jurassic Carmel Limestone examples (fig. 9). Birdseye fenestrae in the stromatolitic rocks of lithofacies B are also commonly filled with anhydrite (fig. 8).

Matrix recrystallization is the rule in the intertidally deposited rocks of lithofacies C. These packstones and grainstones originally contained interstitial mud. Gradational contacts between grains and matrix crystals, uniform crystal size, and patches of unaltered mud are evidence for the formation of pseudospar. Recrystallization is also indicated by the wide separation of initially grain-supported allochems, now floating in more matrix spar than would have normally grown between them. If the interstitial material had been originally spar it would have filled only the intergranular voids, but neomorphic growth of pseudospar from micrite could have expanded the matrix producing the floating grains (fig. 12). Folk (1974) reported that microspar and pseudospar apparently form in a diagenetic environment low in magnesium ions, while unaltered micrite is a stable product in a magnesium-rich environment. Such an interpretation explains the presence of neomorphic spar in lithofacies C, for these rocks are interpreted to have been deposited under normal marine salinities.

Allochem recrystallization, commonly observed in thin sections of lithofacies C and F, was probably controlled by their original composition. Bivalves show variation in recrystallization of inner and outer valve margins that was probably controlled by variations in original mineralogy. Bryozoans show spar-filled zooecia, but skeletal materials, like associated echinoderm fragments, are rarely altered. Oolites commonly show recrystallized concentric rings but are usually not totally recrystallized (fig. 25).

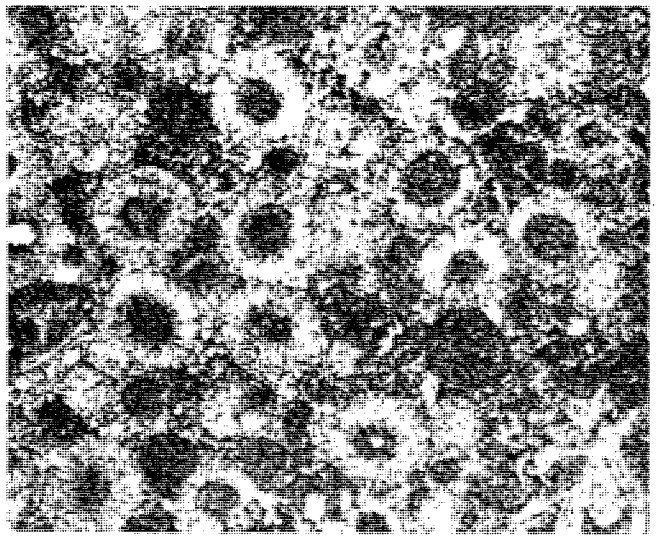

FIGURE 25.–Photomicrograph of partially recrystallized oolites from section 1, unit 19, X8.

### Dolomitization

Rocks of lithofacies B are interpreted, in subsequent parts of this report, to represent deposition in a supratidal zone of a low-energy carbonate shoreline. Modern dolomitization processes have been found to occur in various environments throughout the tropics. The main process of dolomitization involves replacement of primary calcite, and especially aragonite, by reaction with magnesium-rich groundwater. Such water accumulates in areas isolated from normal marine circulation and, in one model, undergoes evaporation sufficient to initiate precipitation of gypsum or anhydrite. When the Mg/Ca ratio approaches 10, replacement of Ca begins (Asquith 1979, p. 21). This produces syngenetic or penecontemporaneous dolomitization.

Two of the most probable models for dolomitization and movement of the Mg-rich brines that caused the dolomitization are–

1. the seepage reflux model, which postulates downward descending supersaline brines (Deffeyes and others 1965), and
2. the evaporative pumping model, in which ascending ground water is enriched in Mg (Hsu and Schneider 1973, p. 417)

As a result of their work in the Abu Dahbi sabka of the Persian Gulf, Hsu and Schneider (1973, p. 421) suggest that pumping from groundwater sources is the most satisfactory model for explaining the movement of Mg-rich brines. The writer believes this is the case of the dolomicrites of the Carmel Formation limestone member, since normal marine limestones overlie the sabka-tidal flat dolomites.

Dolomite of lithofacies B meets the criteria for syngenetic dolomitization, as described by Asquith (1979, p. 22). The individual grain size is very fine, generally less than 10$\mu$. The fabric is sucrosic, and the matrix is uniformly replaced. Evaporitic anhydrite is found within the rocks. No fossils are found within the dolomite, suggestive of conditions of hypersalinity. Stromatolitic bedding is also found. Dolomitization is uniform, and quartz grains generally occur within the rocks (fig. 6).

## DEPOSITIONAL ENVIRONMENTS OF LITHOFACIES

### Lithofacies A

Siliclastic deposition of continental origin combined with possible volcanic-derived deposits characterizes lithofacies A. The underlying Temple Cap Sandstone and clastic rocks of lithofacies A represent the first flush of Jurassic sediments into the trough that extended from Canada into southern Utah (fig. 2). Sandstone in the lower part of the Carmel Formation probably represents reworked Temple Cap Sandstone, for grain sizes and color are similar. The thinly bedded shales and siltstones may represent reworked volcanic material, interpreted as metabentonites by Wright and Dickey (1963, p. 66). Such an origin seems feasible because biotite and sanidine phenocrysts and other glassy material found in the fine clastic units almost certainly indicate a volcanic origin. Most of the volcanic material occurs in a 25-cm to 30-cm bed and may represent an ash fall (Myron Best personal communication December 1980). Matrix of associated sandstone is clay, which further suggests an ash fall or bentonite in this clastic sequence. Other quartz sand-

stone overlies the siltstone and shale of possible volcanic material and may represent sediments eroded from an igneous source to the south or west (Stanley and others 1971, fig. 3, p. 13). The cement in these latter beds is calcite rather than clay as in the sandstone beneath.

Origin of the volcanic material is questionable. The possible ash may have been derived from volcanic activity as far away as northern California, for volcanic activity was noted there by Imlay (1956, fig. 2, plate 8) and Stanley and others (1971, p. 13). The ash may have been carried to southern Utah by northwesterly winds, a direction well documented by associated older and younger eolian deposits (Bigarella 1972, p. 56). However, the sharp clear corners of the biotite phenocrysts suggest that transportation has been minimal and that a source is nearby (Revell Phillips personal communication January 1981).

Lithofacies B

*Dolomicrite Subfacies*

The dolomicrite of lithofacies B represents the beginning of carbonate sedimentation in the southern part of the Carmel seaway. Dolomitic siltstone at the base of the lithofacies signals the end of dominantly siliclastic sedimentation in the Carmel limestone member. That deposition had marked initial development of the trough that extended through central Utah and into southern Utah during the Middle Jurassic. Clastic quartz grains, however, continued to be swept in and mixed with the fine-grained carbonate deposits throughout the supratidal area of this subfacies (fig. 26).

Dolomicrites of the lower Carmel Formation represent sedimentation in a low-energy, shallow-water, hypersaline, supratidal to subtidal environment. Laminations vary from irregular to rippled to cryptalgal as current energy and algal growth changed. Figure 5 shows characteristic current-laminated, quartz-rich, dolomicrite from unit 12 of section 3, and figure 7 shows wavy cryptalgal bedding from units 13 of section 7. Deposition of the thinly laminated dolomicrite occurred in very shallow, quiet water, probably moved by weak tidal currents. Ripple marks were formed (fig. 23) where current energy was moderate.

Cryptalgal dolomicrites, without fenestrae but with wavy irregular bedding, are common to deposits formed in the supratidal zone of ancient and modern carbonate flats (Lucia 1972, p. 188). These Carmel dolomicrites are probably similar to stromatolitic boundstones but have thin discontinuous algal films because of either infrequent inundation or exposure.

*Stromatolitic Boundstone Subfacies*

Algal stromatolites are considered to be the most diagnostic organic features of carbonate tidal-flat sediments (Lucia 1972, p. 162). Stromatolites have been divided into numerous types, both geometric and generic, but the fundamental processes which characterize them and the resulting boundstone are simple. Colonies of coccoid and filamentous blue green algae, in mounds and rubbery mats, trap on their sticky, mucilaginous surfaces sediment washed over them by tides or storms. As successive layers of sediment are added, the algal mat thickens, and new algae grow on the upper surface. In fact, recent experiments have shown that algal mats buried by several millimeters of sediment can reform their upper surface in less than one day (Ginsburg and others 1972, p. 121). Modern algal mats are spatially confined by the limits of alternate wetting and drying. Therefore, they are primarily found in high intertidal to low supratidal environments (Lucia 1972, p. 162).

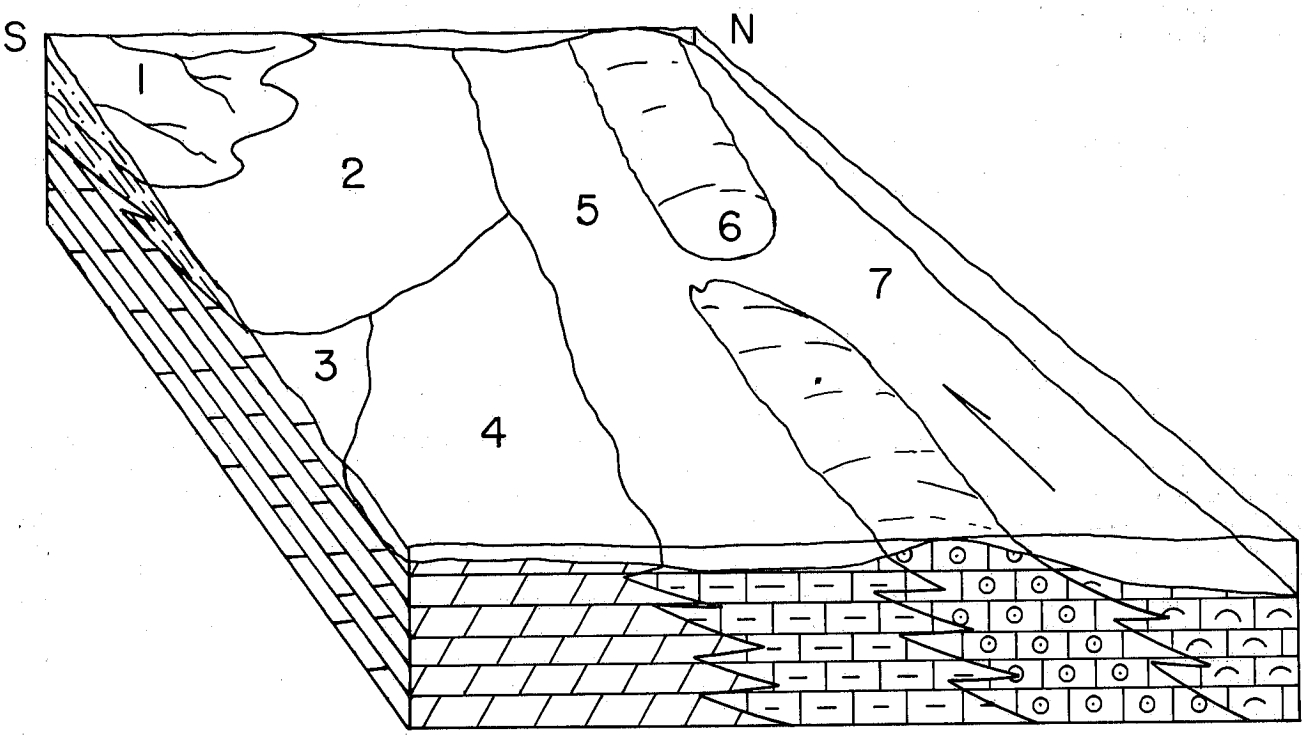


FIGURE 26.—Depositional model for the Carmel Limestone Member: (1) redbeds of banded member, (2) shale of lithofacies D, (3) supratidal anhydrite and stromatolites of lithofacies B, (4) dolomicrite of lithofacies B, (5) argillaceous mudstone of lithofacies E, (6) oolite skeletal packstone of lithofacies C, (7) wackestone of lithofacies C. Arrow points in the direction of current flow.

Stromatolitic boundstones of the Carmel Limestone are similar to most other algal-mat carbonates in that the original algal filaments are not preserved. The rocks do have a layered fabric of trapped intraclasts that were washed onto the algal surface. Coarse-grained accumulations, common in many ancient and modern stromatolite deposits, are not found in the Carmel Limestone beds, probably because of the dampening of wave energy in the shallow, broad, southern tip of the Carmel seaway (fig. 26). Birdseye and laminoid fenestrae in the subfacies are like those in modern algal mats and probably resulted from desiccation of gas heave from decaying organic matter like those described by Wilson (1975, p. 82).

*Evaporite Subfacies*

The presence or absence of evaporites in the supratidal environment is controlled by climate. For example, sabkas in the arid Persian Gulf have evaporite deposits, but those in the more humid Bahama Islands do not (Asquith 1979, p. 40). Evaporation in an arid climate concentrates surface brines and initiates upward capillary movement from the water table (Bathurst 1971, p. 533). The resulting high salinity encourages the precipitation of gypsum and/or anhydrite, which in turn raises the Mg=Ca ratio, causing subsurface dolomitization.

Anhydrite is locally abundant in sediments above older algal mats of Abu Dhabi along the Trucial Coast of the Persian Gulf (Shearman 1978, p. 8). The water table of the sabka generally lies at about the level of the buried algal mats, and it appears that the nodular anhydrite forms in sediments of the capillary zone. Anhydrite occurs in the Carmel subfacies as nodules in a chicken-wire fabric of dolomicrite and as fillings in the fenestrae of the stromatolitic boundstone subfacies. It is likely that nodular anhydrite in Carmel Limestone beds represents supratidal or sabka deposition (fig. 26).

Lithofacies C

Skeletal limestone of lithofacies C documents normal open marine conditions as the Carmel seaway continued its southward transgression. Normal marine salinities are indicated by abundant echinoderm fragments. These intertidal to subtidal rocks are the earliest Carmel beds to document major marine transgression. The fossiliferous oolite sequence immediately overlies the supratidal sabka rocks.

The oolite-skeletal packstone and grainstone subfacies was deposited on oolite shoals (fig. 26). Current energy was moderately high, as suggested by medium-scale cross-bedding. These shoals must have been exposed to moderate wave energy, for the grains are abraded, and fine mud had been winnowed away. Modern examples of such exposed lime sands are found in the keys that dot shoals throughout the Bahama Islands and the Caribbean Sea area.

The bivalve wackestone subfacies represents deposition in a lower-energy subtidal environment. These wackestones overlie the oolite skeletal subfacies and mark the maximum transgression of the Carmel Seaway in this area (fig. 26). Organic activity, mostly by bivalves, was high, because these sediments are burrowed and lack bedding. Occasional isolated crinoid fragments or oolites in the wackestone may represent transportation by a slightly higher-energy regime within the area of deposition of these muddy carbonate sediments. The deeper water along the axis of the Persian Gulf, where carbonate mud with minor skeletal and terrigenous material is accumulating (Heckel 1972, p. 254), is similar to conditions visualized for deposition of the wackestone of lithofacies C.

Lithofacies D

Shale of lithofacies D was deposited on top of the oolitic skeletal limestone of lithofacies C as regression of the Carmel sea began. These fine clastic rocks represent a quiet, shallow-water environment protected from wave energy by oolite shoals (fig. 26). Evidence of organic activity is absent in the area of shale deposition. The lack of fossils may indicate extreme variations of salinities and temperature. The lack of current-generated sedimentary structures indicates that water in which this lithofacies was deposited was sufficiently calm to allow the fine sediments to settle. Because the lithofacies includes the lower deposits of a northward prograding shoreline, the source area was probably to the south or southesat.

Lithofacies E

Alternating deposition of fine terrigenous clastic and calcareous sediments produced the laminated marl of lithofacies E. These light colored lime muds probably were deposited in quiet, protected water near the shoreline (fig. 26). Hypersaline conditions persisted into environments of deposition of lithofacies E. No body fossils nor trace fossils were found in these rocks. As the Carmel seaway withdrew northward, the thin laminated muds began to interfinger with the peloidal grainstones of lithofacies F as the shoreline facies prograded northward.

Lithofacies F

Lithofacies F represents a return to nearly normal marine deposition of peloidal grainstones and supratidal deposition of stromatolitic boundstones and minor evaporites as the Carmel sea reinvaded the area a second time. This reinvasion and reduced salinities are suggested by the presence of bivalves and gastropods. Energy levels for deposition of lithofacies F were greater in the Carmel Junction area than during deposition of the previous two lithofacies, as indicated by micro-laminated peloidal grainstones. Gastropods, such as those found in section 5, were most likely responsible for pascichnid trace fossils found near section 1. Coquinas of bivalves, washed together in death assemblage, occur irregularly throughout the upper cliff of the lithofacies. Figure 28 shows a coquina of bivalves of this lithofacies exposed in the Spring Hollow area, just north of Carmel Junction. Ripple marks are also found in upper beds of lithofacies F (fig. 27).

With the final retreat of the Carmel sea from this area, carbonate deposition ended and the sandy-silty tidal-flat to subaerial redbeds of the Carmel banded member were deposited over the limestone member (fig. 26).

## DEPOSITIONAL SUMMARY

The Carmel Formation limestone member in the Carmel Junction area is characterized by three depositional phases (fig. 29). The combined terrigenous lower redbeds of lithofacies A, the supratidal-sabka dolomicrites of lithofacies B, and the oolite packstones and grainstones of lithofacies C represent the transgressive first phase (fig. 29A). The prograding shale of lithofacies D and the argillaceous mudstone of lithofacies E represent regressive phase two (fig. 29B). The transgressive third phase of deposition is represented by the peloidal grainstone of lithofacies F (fig. 29C). Figure 30 displays graphs showing the transgressive-regressive depositional phases and energy levels of the Carmel Limestone Member.

Supratidal and intertidal rocks of the first phase mark the southward advance of the Carmel seaway (fig. 29A). This ad-

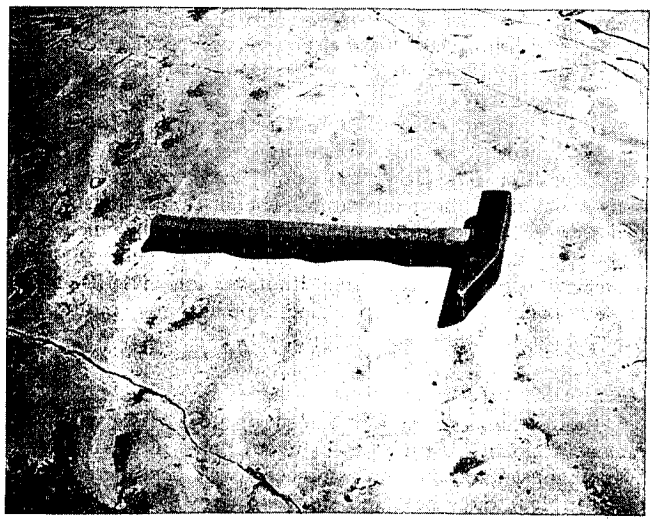

FIGURE 27.–Ripple marks at the top of lithofacies F in the Spring Hollow area.

vance was probably triggered by downwarping of the Rocky Mountain geosynclinal trough through Idaho and into central and southern Utah prior to, and contemporary with, uplift of the Sevier Arch to the west (Armstrong 1968, p. 451). The Sevier arch and area to the south are probably the source for clastic sediments and volcanic material found in lithofacies A. Lithofacies B marks the beginning of carbonate deposition and a decrease of clastic influx. At this time, the Carmel sea in southern Utah was probably very shallow and well oxygenated as indicated by the light colored, thinly laminated dolomite. The environments were too saline for organisms other than algae, as suggested by the lack of fossils other than stromatolites. Scattered horizons of ripple marks indicate gentle currents. Early dolomitization of the carbonate sediments and precipitation of gypsum and anhydrite resulted from evaporation and elevated salinities in restricted ponds or lagoons in the generally arid shoreline area.

As the sea continued its southward advance and the shoreline receded, normal marine conditions existed in the Carmel Junction area. Formation of oolite shoals suggests that currents were moderately rigorous at times along the shoreline. Terrigenous siltstone units interfinger with the cross-bedded packstones and grainstones and probably accumulated in water quiet enough that fine sediments were deposited and not washed away. The bioturbated bivalve wackestone subfacies of lith-

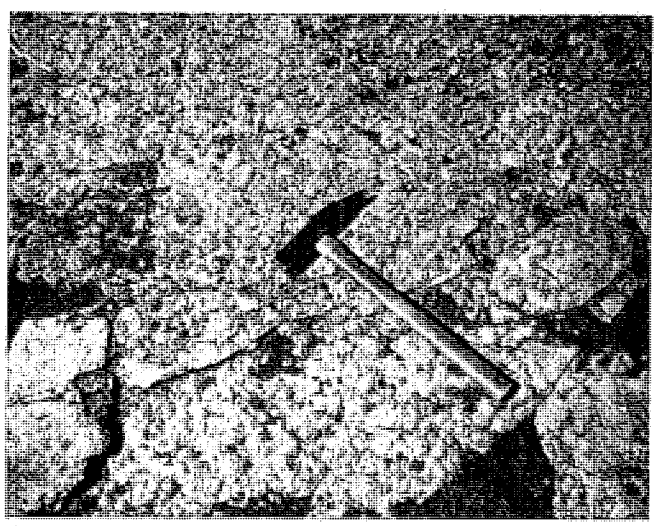

FIGURE 28.–Bivalve coquina at top of lithofacies F in the Spring Hollow area, north of Carmel Junction.

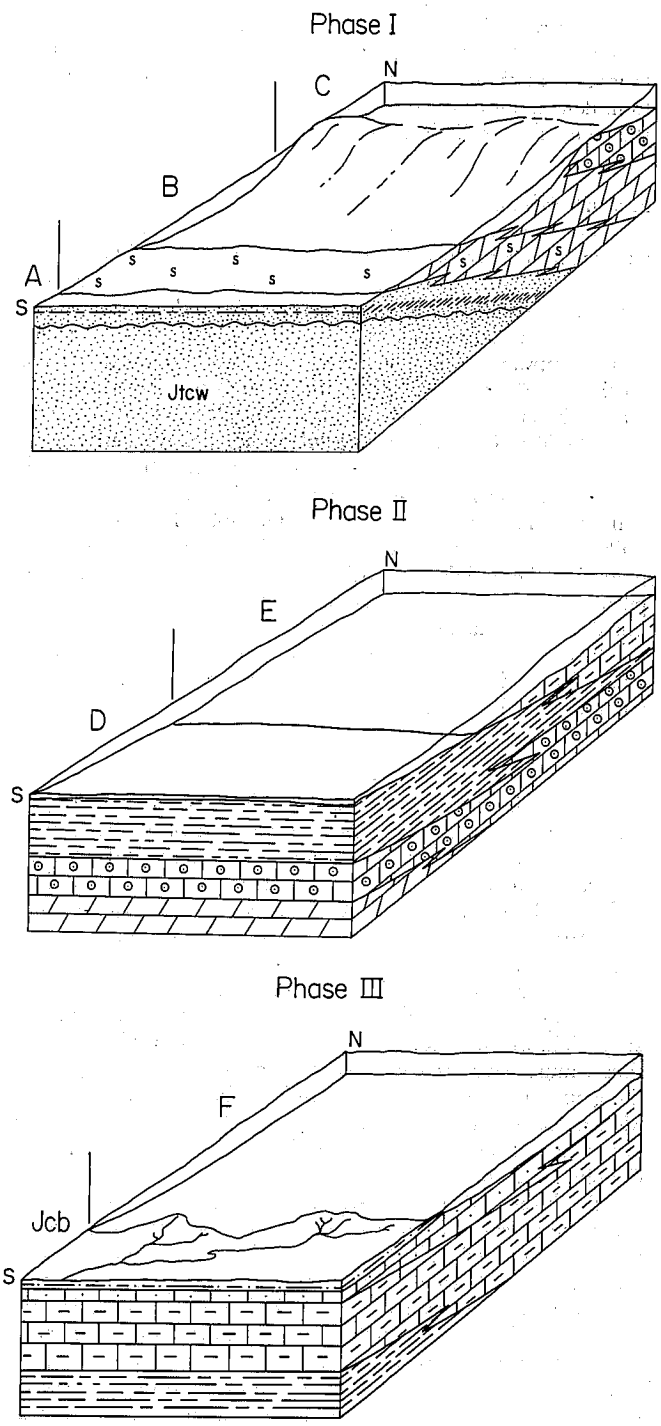


FIGURE 29A.–Transgressive oolite shoals of phase I, Carmel limestone member. B.–Regression of sea and prograding shale of phase II of Carmel limestone member. C.–Minor transgression of peloidal grainstones of phase III of Carmel limestone member.

ofacies C represents deeper-water deposition in the Carmel Sea. These carbonate muds accumulated in quiet water so that the substrate was suitable for organic life. Oolites and echinoderm fragments found in the wackestone probably represent spillover from the shoals during high-energy storm surges.

The second main phase of deposition began as the fine, terrigenous, clastic muds of lithofacies D prograded abruptly over the oolite sequence, as the Carmel sea regressed northward (fig. 29B). These sediments probably were derived from sources to the south or southeast and were washed out into the lagoonal area and settled out of the very quiet waters. Carbonate sediments combine with interfingering argillaceous material to form the thinly laminated mudstone of lithofacies E. Hypersaline conditions existed as these two lithofacies were deposited, for virtually no fossils are found in these rocks.

The peloidal grainstones, stromatolitic boundstones, and evaporites of lithofacies F mark third-phase deposition and a limited reinvasion of the Carmel sea into the area (fig. 29C). Normal marine conditions are suggested by the presence of bivalves and gastropods that inhabited the fine carbonate muds of the sea floor. Times of shallow, hypersaline water are represented by evaporites and stromatolitic boundstone. Silty clastic beds found in the middle of the lithofacies represent a minor change when continental sedimentation exceeded carbonate sedimentation. Bivalve coquinas and ripple marks at the top of lithofacies F suggest a shallowing of the Carmel seaway as it withdrew from the southern part of Utah. The tidal-flat and subaerial red beds of the banded member were deposited on top of the limestone member of the Carmel Formation.

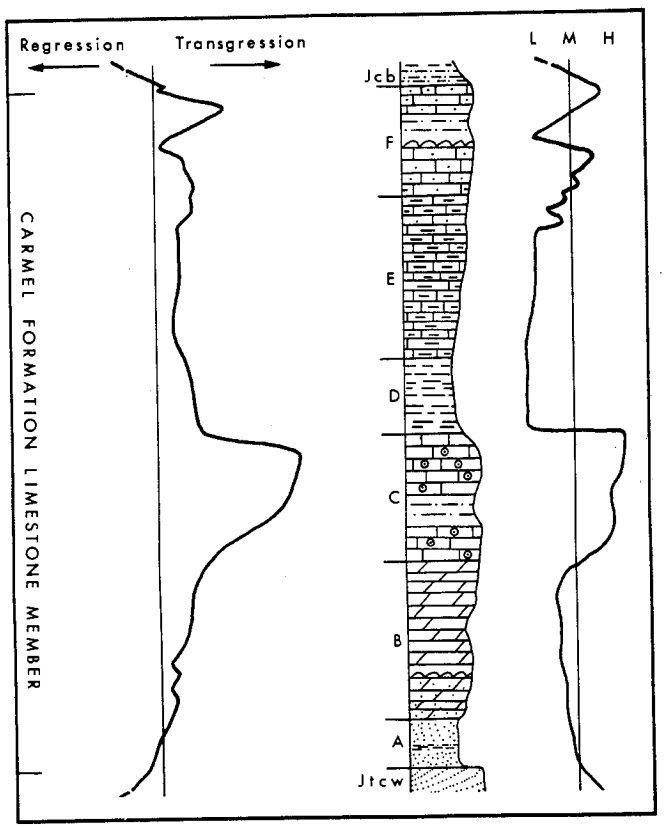


FIGURE 30.–Generalized stratigraphic column of limestone member with transgressive-regressive curve on the left and energy level (Low, L; Medium, M; and High, H) curve on the right.

## PETROLEUM POTENTIAL

Current production of petroleum from correlative rocks (Twin Creek Limestone) in southwestern Wyoming leaves little doubt as to the potential of the other marine limestone deposited by the Middle Jurassic sea, including the limestone member of the Carmel Formation. Similar Jurassic rocks in the Texas-Louisiana region are known to contain 15 million barrels of oil (Bishop 1968). Some of the rich reservoirs of Saudi Arabia have been producing tremendous quantities of oil for nearly 40 years out of Jurassic carbonates deposited from the ancient Tethys Sea (Powers 1961). In fact, over 25 percent of the world's petroleum production is from carbonate rocks.

In light of recent drilling in central Utah and according to Floyd Moulton (personal communication January 1981), Jurassic marine rocks capable of producing vast amounts of petroleum lie in a belt 32 km (20 mi) wide in west central Utah. Rocks of lithofacies B and C, if found in the subsurface to the north and northeast in a structural or stratigraphic trap where hydrocarbons accumulate, could be highly productive.

## APPENDIX

Section 1: Located on the east side of U.S. 89 about 200 m south of Carmel Junction, in the NW ¼ of section 30, T. 41 S, R. 7 W, in Kane County, Utah.

| *Unit* | *Description* | *Thickness Unit* | *Cumulative (meters)* |
|---|---|---|---|
| | Carmel Formation, banded member: interbedded siltstone and sandstone, light red to light gray, slope former. | | |
| | Carmel Formation, limestone member. | | |
| | Lithofacies E | | |
| 31 | Grainstone, light olive gray, peloidal, vuggy, bivalve coquinas 2 to 3 cm thick towards top, massive cliff former. | 3.7 | 71.1 |
| 30 | Siltstone, brownish yellow, argillaceous, slope former. | 1.2 | 67.4 |
| 29 | Grainstone, yellowish gray, peloidal, vuggy, ledge former. | .5 | 66.2 |
| 28 | Siltstone, brownish yellow, argillaceous, slope former. | 2.1 | 65.7 |
| 27 | Grainstone, yellowish gray, peloidal, undulatory bedded with silt partings, cliff former. | 3.6 | 63.6 |
| 26 | Grainstone, yellowish gray, peloidal, silty, undulatory bedded with beds up to 2 cm thick, nonresistant ledge-former. | .2 | 60.0 |
| 25 | Sitlstone, brown, argillaceous, slope former. | 2.1 | 59.8 |
| 24 | Grainstone, yellowish gray weathers the same, peloidal, ledge former. | .4 | 57.7 |
| | Lithofacies E | | |
| 23 | Mudstone, light olive gray, argillaceous, thinly bedded, ledgy slope former. | 19.2 | 57.3 |
| | Lithofacies D | | |
| 22 | Shale, reddish purple to grayish green, poorly exposed, slope former. | 13.2 | 38.1 |
| | Lithofacies C | | |
| 21 | Wackestone, light olive gray, abundant bioclasts of bivalve and crinoid material, burrowed, forms nonresistant slope but rock outcrops to the south about 10 m. | 2.1 | 24.9 |
| 20 | Packstone, light olive gray, contains oolites, crinoid and bivalve material, cross-bedded, ledge former. | 1.5 | 22.8 |
| 19 | Packstone, brownish gray, contains clay intraclasts, oolites, slope former. | .2 | 21.3 |
| 18 | Grainstone, yellowish gray, weathers the same, larger oolites with some bi- | 1.7 | 21.1 |

| | | | |
|---|---|---|---|
| | valve and crinoid material present, ledge former. | | |
| 17 | Packstone, yellowish gray, oolitic, undulatory bedded, ledge former. | 1.0 | 19.4 |
| 16 | Siltstone, grayish brown, argillaceous, limy, slope former. | 5.7 | 18.4 |
| 15 | Grainstone, dark yellowish brown, weathers yellowish gray, abundant fossil material of bivalves, crinoids, bryozoans, undulatory bedded with oolites throughout, forms ledgy slope. | .65 | 12.7 |
| | Lithofacies B | | |
| 14 | Siltstone, yellowish brown, dolomitic, slope former. | 1.5 | 12.05 |
| 13 | Mudstone, light grayish yellow, weathers grayish yellow, laminations up to 3 cm thick, dolomitic, ledge former. | .7 | 10.55 |
| 12 | Mudstone, light grayish yellow, weathers the same, dolomitic, grades into 13, cliff former. | 1.9 | 9.85 |
| 11 | Stromatolitic boundstone, grayish yellow, crinkly algal structures, dolomitic, ledge former. | .25 | 7.95 |
| 10 | Mudstone, light yellowish gray, dolomitic, thinly laminated, ledge slope former. | .6 | 7.7 |
| 9 | Mudstone, light grayish yellow, dolomitic, silty, thinly bedded, numerous brown blebs in the matrix, massive cliff former. | 2.8 | 7.1 |
| 8 | Siltstone, light grayish pink, weathers pale red, dolomitic, laminae up to 3 cm thick, grades into 9, cliff former. | .8 | 4.3 |
| | Lithofacies A | | |
| 7 | Sandstone, pale purplish to red, very fine grained, massive, 4 cm greenish gray sandstone beds crop out near the top, high slope former. | .3 | 3.5 |
| 6 | Sandstone, alternating pale red to greenish gray laminations, beds up to 5 cm thick, upper 20 cm are calcareous, ledge former. | .35 | 3.2 |
| 5 | Shale, dark reddish purple, lenticular bedded, silty in places, slope former. | .2 | 2.85 |
| 4 | Sandstone, alternating greenish gray to pale red, medium grained, friable, porous, high slope former. | .8 | 2.65 |
| 3 | Sandstone, purplish red, tuffaceous, biotite and sanidine phenocrysts, very fine grained, becomes more silty near the top of unit, platy weathering, slope former. | .25 | 1.85 |
| 2 | Sandstone, yellow brown, grades to greenish gray, medium grained, thinly bedded, ledge former. | .1 | 1.6 |
| 1 | Sandstone, light greenish gray, medium grained, massive, very porous and friable, contains green clay in the matrix, thin laminae of greenish gray shale in the lower part, high slope former. | 1.5 | 1.5 |
| | Total limestone member | | 71.1 |
| | Temple Cap Sandstone, White Throne Member: sandstone, light gray, well sorted, cross-bedded, cliff former. | | |

Section 4: Located in the SE ¼ of section 25, T. 41 S, R. 8 W, and in the SW ¼ of section 30, T. 41 S, R. 7 W, where the limestone member of the Carmel Formation is well exposed in a roadcut.

| *Unit* | *Description* | *Thickness Unit* | *Cumulative (meters)* |
|---|---|---|---|
| | Carmel Formation, banded member: interbedded siltstone and sandstone, light red to light gray, slope former. | | |
| | Carmel Formation, limestone member | | |
| | Lithofacies F | | |
| 25 | Grainstone, yellowish gray, peloidal, bivalve coquina 2 cm thick in the middle of unit, vuggy, cliff former. | 6.2 | 66.38 |
| 24 | Sandstone, greenish white, medium grained, calcareous, slope former. | 1.0 | 60.18 |
| 23 | Siltstone, light yellowish brown. | 1.1 | 59.18 |
| 22 | Shale, greenish brown, slope former. | .3 | 58.08 |
| 21 | Grainstone, light brownish gray, weathers light gray, vuggy, peloidal ledge and cliff former. | 4.2 | 57.78 |
| | Lithofacies E | | |
| 20 | Mudstone, light grayish brown, argillaceous thinly laminated, ledge former. | 18.7 | 53.58 |
| 19 | Interbedded sandstone and siltstone, yellowish brown to greenish white, megaripples at base, cliff former. | 1.3 | 34.88 |
| | Lithofacies D | | |
| 18 | Shale, reddish purple to greenish gray, silty, poorly exposed slope former. | 5.0 | 33.58 |
| 17 | Mudstone, olive gray, thinly laminated, ledge former. | 1.3 | 28.58 |
| 16 | Mudstone, light yellowish gray, dolomitic, ledge former. | .5 | 27.28 |
| 15 | Siltstone, pale red. | .8 | 26.78 |
| 14 | Shale, grayish green to purplish red, slightly calcareous, slope former at base of roadcut. | 2.6 | 25.98 |
| | Lithofacies C | | |
| 13 | Grainstone, yellowish brown, oolitic, bioclasts of bivalve and crinoid material, undulatory bedded, ledge cliff former. | 1.0 | 23.38 |
| 12 | Siltstone, yellowish brown, calcareous slope former. | 3.0 | 22.38 |
| 11 | Grainstone, light olive gray, oolitic, bivalve and crinoid material, intraclasts of green clay, cross-bedded, ledge former. | 4.5 | 19.38 |
| 10 | Mudstone, light olive brown, dolomitic, thin bedded. | .23 | 14.88 |
| 9 | Grainstone, yellowish gray, massive, bioclasts of bivalves and crinoids, ledge former. | .6 | 14.65 |
| | Lithofacies B | | |
| 8 | Mudstone, light olive brown, dolomitic, massive, cliff former. | .9 | 14.05 |
| 7 | Siltstone, grayish brown, argillaceous, slope former. | 2.3 | 13.15 |
| 6 | Mudstone, yellowish gray, weathers the same, dolomitic, thinly bedded, ledge former. | 1.25 | 10.85 |
| 5 | Siltstone, brown, argillaceous, slope former. | .9 | 9.6 |
| 4 | Mudstone, grayish yellow, weathers the same, dolomitic, vuggy, thin bedded, cliff former. | .5 | 8.7 |
| 3 | Mudstone, light grayish yellow, silty, dolomitic, two oxidized beds 4 cm thick, crop out at the base, massive cliff former. | 1.8 | 8.2 |
| 2 | Siltstone, light grayish pink, weathers pale red, thinly bedded, cliff former. | 1.4 | 6.4 |
| | Lithofacies A | | |
| 1 | Interbedded sandstone, siltstone, and shale, greenish white to purplish red, poorly exposed slope zone at base of limestone member. | 5.0 | 5.0 |
| | Total limestone member | | 66.38 |
| | Temple Cap Sandstone, White Throne Member: sandstone, light gray, well sorted, medium grained, cross-bedded, cliff former. | | |

## REFERENCES CITED


Armstrong, R. L., 1968, Sevier orogenic belt in Nevada and Utah: Geological Society of America Bulletin, v. 29, p. 429–58.

Asquith, G. B., 1979, Subsurface carbonate models: A concise review: Petroleum Publishing, Tulsa, Oklahoma, 120p.

Bagshaw, L. H., 1977, Paleoecology of the lower Carmel Formation of the San Rafael Swell, Emery County, Utah: Brigham Young University Geology Studies, v. 24, pt. 2, p. 51–62.

Baker, A. A., Dane, C. H., and Reeside, J. B., 1936, Correlation of the Jurassic formations of parts of Utah, Arizona, New Mexico, and Colorado: U.S. Geologic Survey Professional Paper 183, 66p.

Bathurst, R. G. C., 1971, Carbonate sediments and their diagenesis: Developments in sedimentology, Elsevier, New York.

Bigarella, J. J., 1972, Eolian environments–their characteristics, recognition, and importance: In Rigby, J. K., and Hamblin, W. K. (eds.), Recognition of ancient sedimentary environments: Society of Economic Paleontologists and Mineralogists, Special Publication no. 16, p. 12–62.

Bishop, W. F., 1968, Petrology of upper Smackover Limestone in North Haynesville field, Clairborne Parish, Louisiana: American Association of Petroleum Geologists Bulletin, v. 52, no. 1, p. 92–128.

Cashion, W. B., 1967, Carmel Formation of the Zion Park region southwestern Utah–a review: U.S. Geological Survey Bulletin 1244-J, 9p.

———, 1967, Geology of the south flank of the Markagunt Plateau, northwest Kane County, Utah: United States Geological Survey Miscellaneous Geologic Investigations, Map I-494.

Deffeyes, K. S., Lucia, F. J., and Weyl, P. K., 1965, Dolomitization of recent Plio-Pleistocene sediments by marine evaporite waters on Bonaire, Netherlands Antilles: In Pray, L. C., and Murray, R. C. (eds.), Dolomitization and limestone diagenesis, a symposium: Society of Economic Paleontologists and Mineralogists Special Publication no. 13, 180p.

Dunham, R. J., 1962, Classification of carbonate rocks according to depositional texture: In Ham, W. E. (ed.), Classification of carbonate rocks, a symposium: American Association of Petroleum Geologists Memoir 1, 279p.

Folk, R. L., 1974, The natural history of crystalline calcium carbonate, effect of magnesium content and salinity: Journal of Sedimentary Petrology, v. 44, p. 40–53.

Friedman, G. M., 1949, Identification of carbonate minerals by staining methods: Journal of Sedimentary Petrology, v. 29, p. 87–97.

Geesaman, R. C., and Voorhees, B. J., 1980, Facies and depositional tectonics of Middle Jurassic Carmel Formation, southern Utah: American Association of Petroleum Geologists Bulletin, v. 64, no. 5, p. 712.

Gilluly, J., and Reeside, J. B., Jr., 1928, Sedimentary rocks of the San Rafael Swell and some adjacent areas in eastern Utah: U.S. Geological Survey Professional Paper 140-D, p. 61–110.

Ginsburg, R. N., Rezak, R., and Wray, J. L., 1972, Geology of calcareous algae: Sedimenta 1, University of Miami, Miami, Florida, 66p.

Gregory, H. E., 1950, Geology and geography of the Zion Park region, Utah and Arizona: U.S. Geological Survey Professional Paper 220, 200p.

Heckel, P. H., 1972, Recognition of ancient shallow marine environments: In Rigby, J. K., and Hamblin, W. K. (eds.), Recognition of ancient sedimentary environments: Society of Economic Paleontologists and Mineralogists, Special Publication no. 16, p. 226–86.

Hsu, K. J., and Schneider, J., 1973, Progress report on dolomitization hydrology of Abu Dhabi sabkas, Arabian Gulf: In Purser, B. H. (ed.), The Persian Gulf: Holocene sedimentation and diagenesis in a shallow epicontinental sea: Springer-Verlag, New York, p. 409–22.

Imlay, R. W., 1952, Correlation of the Jurassic formations of North America, exclusive of Canada: Geological Society of America Bulletin, v. 63, p. 953–52.

———, 1957, Paleoecology of Jurassic seas in the western interior of the United States: Geological Society of America Memoir 67, p. 469–504.

———, 1964, Marine Jurassic pelecypods from central and southern Utah: U.S. Geological Survey Professional Paper 483-C, 42p.

———, 1967, Twin Creek Limestone (Jurassic) in the western interior of the United States: U.S. Geological Survey Professional Paper 540, 105p.

Kerr, S. D., Jr., and Thomson, A., 1963, Origin of nodular and bedded anhydrite in Permian shelf sediments, Texas and New Mexico: American Association of Petroleum Geologists Bulletin, v. 47, p. 1726–32.

Logan, B. W., Rezack, R., and Ginsburg, R. N., 1964, Classification and environmental significance of algal stromatolites: Journal of Geology, v. 12, p. 68–83.

Lowrey, R. O., 1976, Paleoenvironment of the Carmel Formation at Sheep Creek Gap, Daggett County, Utah: Brigham Young University Geology Studies, v. 23, pt. 1, p. 175–203.

Lucia, F. J., 1972, Recognition of evaporite-carbonate shoreline sedimentation: In Rigby, J. K., and Hamblin, W. K. (eds.), Recognition of ancient sedimentary environments: Society of Economic Paleontologists and Mineralogists, Special Publication No. 16, p. 160–91.

McKee, E. D., and others, 1956, Paleotectonic maps of the Jurassic System: U.S. Geological Survey Miscellaneous Geological Investigations, Map I-175.

Moore, R. C., 1953, Treatise on invertebrate paleontology: Bryozoa, part G: Geological Society of America, 253p.

———, 1966, Treatise on invertebrate paleontology: Echinodermata 3, part U: Geological Society of America, 366p.

Peterson, J. A., 1972, Jurassic System: In Geologic atlas of the Rocky Mountain region: Rocky Mountain Association Geologists, 331p.

Peterson, F., and Pipiringos, G. N., 1979, Stratigraphic relation of the Navajo Sandstone to Middle Jurassic formations, southern Utah and northern Arizona: U.S. Geological Survey Professional Paper 1035-B, 43p.

Powell, J. W., 1875, Exploration of the Colorado River of the West and its tributaries: Government Printing Office, Washington, D.C., p. 190.

Powers, R. W., 1962, Arabian upper Jurassic carbonate reservoir rocks: In Ham, W. E. (ed.), Classification of carbonate rocks, a symposium: American Association of Petroleum Geologists, Memoir 1, p. 122–92.

Seilacher, A., 1967, Bathymetry of trace fossils: Marine Geology, v. 5, p. 413–28.

Shearman, D. J., 1978, Evaporites of coastal sabkhas: In Dean, W. E., and Schreibner, B. C. (eds.), Marine evaporites: Society of Economic Paleontologists and Mineralogists Short Course No. 4, 188p.

Sohl, N. F., 1965, Marine Jurassic gastropods, central and southern Utah: U.S. Geological Survey Professional Paper 503-D, 29p.

Stanley, K. O., Jordon, W. M., and Dott, R. H., Jr., 1971, New hypothesis of Early Jurassic paleogeography and sediment dispersal for western United States: American Association of Petroleum Geologists Bulletin, v. 55, p. 10–19.

Stokes, W. C., and Heylum, E. B., 1965, Tectonic history of south central Utah: In Geology and resources of south central Utah–Resources for power: Utah Geological Society Guidebook to Geology of Utah, no. 19, p. 3–11.

Thompson, S. E., and Stokes, W. L., 1970, Stratigraphy of the San Rafael Group, southwest and south central Utah: Utah Geological and Mineral Survey Bulletin 87, 53p.

Wilmarth, M. G., 1938, Lexicon of geologic names of the United States: U.S. Geological Survey Bulletin 896, p. 350–51.

Wilson, J. L., 1975, Carbonate facies in geologic history: Springer-Verlag, New York, 471p.

Wright, J. C., and Dickey, D. D., 1963, Relations of the Navajo and Carmel Formations in southwest Utah and adjoining Arizona: U.S. Geological Survey Professional Paper 450-E, p. 63–67.

———, 1978, Miscellaneous cross sections of the Jurassic San Rafael Group in southern Utah: U.S. Geological Survey Open-file Reports 78-965 and 966.

———, 1979, Measured stratigraphic sections of Jurassic San Rafael Group and adjacent rocks in Kane County, Utah: U.S. Geological Survey Open-file Report 79-1373, p. 36–43.